PLOS GENETICS

RESEARCH ARTICLE

G protein-coupled estrogen receptor regulates embryonic heart rate in zebrafish

Shannon N. Romano[1], Hailey E. Edwards[1], Jaclyn Paige Souder[1], Kevin J. Ryan[1], Xiangqin Cui[2¤], Daniel A. Gorelick[1]*

1 Department of Pharmacology & Toxicology, University of Alabama at Birmingham, Birmingham, Alabama, United States of America, **2** Department of Biostatistics, University of Alabama at Birmingham, Birmingham, Alabama, United States of America

¤ Current address: Department of Biostatistics and Bioinformatics, Emory University, Atlanta, Georgia, United States of America
* danielg@uab.edu

OPEN ACCESS

Citation: Romano SN, Edwards HE, Souder JP, Ryan KJ, Cui X, Gorelick DA (2017) G protein-coupled estrogen receptor regulates embryonic heart rate in zebrafish. PLoS Genet 13(10): e1007069. https://doi.org/10.1371/journal.pgen.1007069

Editor: Mary C. Mullins, University of Pennsylvania School of Medicine, UNITED STATES

Received: May 18, 2017

Accepted: October 11, 2017

Published: October 24, 2017

Data Availability Statement: All relevant data are within the paper and its Supporting Information files.

Funding: This work was supported by start-up funds from University of Alabama at Birmingham and by funds from the National Institutes of Health T32GM008111 (to SNR), T32GM008361 (to JPS), and ES026337 (to DAG). The funders had no role in study design, data collection and analysis, decision to publish, or preparation of the manuscript.

Abstract

Estrogens act by binding to estrogen receptors alpha and beta (ERα, ERβ), ligand-dependent transcription factors that play crucial roles in sex differentiation, tumor growth and cardiovascular physiology. Estrogens also activate the G protein-coupled estrogen receptor (GPER), however the function of GPER *in vivo* is less well understood. Here we find that GPER is required for normal heart rate in zebrafish embryos. Acute exposure to estrogens increased heart rate in wildtype and in ERα and ERβ mutant embryos but not in GPER mutants. GPER mutant embryos exhibited reduced basal heart rate, while heart rate was normal in ERα and ERβ mutants. We detected *gper* transcript in discrete regions of the brain and pituitary but not in the heart, suggesting that GPER acts centrally to regulate heart rate. In the pituitary, we observed *gper* expression in cells that regulate levels of thyroid hormone triiodothyronine (T3), a hormone known to increase heart rate. Compared to wild type, GPER mutants had reduced levels of T3 and estrogens, suggesting pituitary abnormalities. Exposure to exogenous T3, but not estradiol, rescued the reduced heart rate phenotype in *gper* mutant embryos, demonstrating that T3 acts downstream of GPER to regulate heart rate. Using genetic and mass spectrometry approaches, we find that GPER regulates maternal estrogen levels, which are required for normal embryonic heart rate. Our results demonstrate that estradiol plays a previously unappreciated role in the acute modulation of heart rate during zebrafish embryonic development and suggest that GPER regulates embryonic heart rate by altering maternal estrogen levels and embryonic T3 levels.

Author summary

Estrogen hormones are important for the formation and function of the nervous, reproductive and cardiovascular systems. Here we report that acute exposure to estrogens increases heart rate, a previously unappreciated function of estrogens. Using zebrafish with mutations in genes that respond to estrogens, we found that heart rate is regulated not by the typical molecules that respond to estrogens–the nuclear estrogen receptors–but

Competing interests: The authors have declared that no competing interests exist.

rather by a different molecule, the G protein-coupled estrogen receptor. We also show that estrogens increase heart rate by increasing levels of thyroid hormone. Our results reveal a new function for the G protein-coupled estrogen receptor and a new connection between estrogens and thyroid hormone. Environmental compounds that mimic estrogens can be harmful because they can influence gonad function. Our results suggest that endocrine disrupting compounds may also influence cardiac function.

Introduction

Zebrafish are an established model for human cardiovascular development and function [1] with conserved estrogen signaling [2–4]. While studying the function of ERα (*esr1*) in zebrafish embryonic heart valves [5, 6], we serendipitously observed that estrogen receptor modulators caused acute changes in heart rate. Estrogens bind two classes of receptors: nuclear hormone receptors (ERα, ERβ) that are ligand-dependent transcription factors [7], and the G protein-coupled estrogen receptor (GPER, also known as GPR30), an integral membrane protein [8, 9]. It has been difficult to tease apart to what degree ERα and/or ERβ are involved in regulating GPER function *in vivo*. The observations that ERα can directly activate G proteins in cultured cells [10–13] and that GPER coimmunoprecipitated with ERα in tumor cells [14] has been used to argue that either GPER is dispensable for estrogen-dependent signaling or that GPER mediates interactions between ERα and G proteins [15]. Studies using GPER-deficient mice implicate GPER in ventricular hypertrophy [16], regulation of blood pressure and vascular tone [17, 18] and atherosclerosis progression [19], but whether nuclear ER signaling is required for GPER function in these contexts is unknown. Additionally, these studies examined GPER function in adult animals, while the role of GPER during embryonic development is not well understood. Here we use zebrafish embryos, an established model of human development, to reveal a new function for GPER during cardiovascular development.

Estrogen signaling often differs between males and females. However, zebrafish embryos and larvae are bipotential hermaphrodites that have not begun to sexually differentiate before approximately 10 days post fertilization (dpf) [20], meaning that estrogen levels are uniform between age-matched embryos. Additionally, zebrafish embryos develop outside of the mother and not within a confined space, such as the uterus. Therefore, zebrafish embryos are not subject to local estrogen concentration gradients, as has been reported to occur in rodents depending upon their position *in utero* and their proximity to embryos of the same or opposite sex [21, 22]. These developmental traits make zebrafish a powerful model to study how sex hormone signaling influences the formation and function of non-gonadal tissues. Using complementary genetic and pharmacologic approaches, we sought to characterize how estradiol regulates heart rate and determine to what extent each estrogen receptor mediates estradiol-dependent changes in heart rate in zebrafish embryos.

Results

Acute estradiol exposure increased heart rate in zebrafish embryos

We exposed 49 hour post fertilization (hpf) embryos to 17β-estradiol (E2) and assayed heart rate following one hour exposure. We found that E2 exposure caused an approximately 20% increase in heart rate (Fig 1, mean difference in heart rate between estradiol and vehicle exposed embryos 26.51 ± 10.63 (standard deviation) beats per minute (bpm); see S1 Table for heart rate values for each embryo in this and subsequent experiments). Exposure to

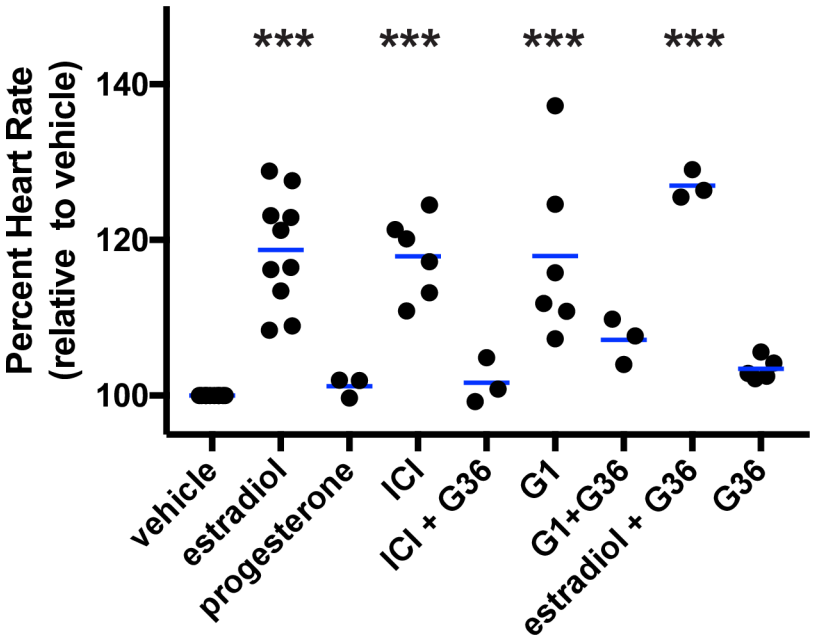

Fig 1. Estradiol and GPER agonists increased heart rate in zebrafish embryos. Wildtype embryos were incubated in water containing vehicle (0.1% DMSO), estradiol (3.67 μM, ER/GPER agonist), progesterone (1 μM), ICI (10 μM ICI182,780, ER antagonist/GPER agonist), G1 (1 μM, GPER agonist), G36 (1 μM, GPER antagonist) or two chemicals in combination at 49 hours post fertilization and heart rates were measured 1 hour following treatment. ***, p<0.0001 compared to vehicle, ANOVA with Dunnett's test. Each black circle represents the mean heart rate from a single clutch of embryos (3–16 embryos per clutch). Horizontal blue lines are the mean of each treatment.

https://doi.org/10.1371/journal.pgen.1007069.g001

progesterone, a structurally similar steroid sex hormone, had no effect on heart rate (Fig 1, mean difference in heart rate 1.57 ± 1.71 bpm), suggesting that the effects on heart rate were specific to estrogens. Our results are consistent with previous results in cultured cells demonstrating that progesterone binds GPER with less than 0.01% binding affinity compared to E2 [23]. However, we cannot exclude the possibility that GPER could respond to higher concentrations of progesterone *in vivo*.

To explore whether heart rate was influenced by nuclear estrogen receptor or GPER signaling pathways, we employed a pharmacological approach. We exposed embryos to ICI182,780 (fulvestrant), a well-characterized ERα and ERβ antagonist [24] that also acts as a GPER agonist [8]. Following one hour exposure to ICI182,780, heart rate was significantly increased (Fig 1, mean difference in heart rate 25.17 ± 9.24 bpm). This effect was blocked by co-administration of G36, a specific GPER antagonist [25] (Fig 1, mean difference in heart rate 2.26 ± 4.09 bpm), suggesting that estradiol increases heart rate via GPER. We also exposed embryos to G1, a specific GPER agonist with no detectable agonist activity against nuclear estrogen receptors [26], and found that heart rate increased significantly (Fig 1, mean difference in heart rate 26.57 ± 15.89 bpm). This effect was partially blocked by co-administration of G36 (Fig 1, mean difference in heart rate 10.95 ± 3.35 bpm). Together, our pharmacological results suggest that GPER regulates heart rate acutely.

Curiously, the GPER inhibitor G36 by itself did not change heart rate significantly (Fig 1, mean difference in heart rate 5.00 ± 2.26 bpm). Additionally, while G36 partially blocked ICI182,780- and G1-dependent increases in heart rate, G36 failed to inhibit estradiol-

dependent increase in heart rate (Fig 1, mean difference in heart rate 39.75 ± 2.87 bpm). This could be due to off-target effects, a limitation of pharmacologic approaches, or due to differences in how G36, which was designed to inhibit human GPER, binds to zebrafish GPER. To definitively test the hypothesis that estradiol regulates heart rate via GPER, we generated *gper* mutant embryos, exposed them to estrogen receptor modulators and assayed heart rate.

gper mutant embryos fail to respond to estrogens and have reduced embryonic heart rate

Using CRISPR-Cas technology [27], we generated embryos with a 133 basepair deletion in the *gper* open reading frame (Fig 2A and 2B; S1 Fig). Embryos were viable and grossly normal, allowing us to measure heart rate (Fig 2C and 2D). We exposed homozygous maternal zygotic *gper* mutant embryos (*MZgper-/-*) to estradiol, to ICI182,780 or to G1 and found no increase in heart rate compared to embryos exposed to vehicle (Fig 2E, mean difference in heart rate estradiol versus vehicle 0.42 ± 11.47, ICI versus vehicle -9.65 ± 12.41, G1 versus vehicle -0.38 ± 0.33). Our results demonstrate that estradiol increases heart rate in a GPER-dependent manner. Note that zygotic *gper* mutants exhibited increased heart rate in response to estradiol (S1 Fig, mean difference in heart rate 29.11 ± 6.16 bpm), indicating that GPER is maternally deposited into oocytes and expressed in embryos. This is consistent with previously published results that detected *gper* transcript in zebrafish embryos at 1 hpf, suggesting the presence of maternally loaded *gper* mRNA [28].

To test whether endogenous estrogens regulate heart rate during embryonic development, we examined basal heart rate in GPER mutant embryos reared in untreated water, reasoning that if heart rate was reduced, then that would suggest that endogenous estradiol regulates heart rate via GPER. We compared heart rate in wildtype versus *MZgper-/-* embryos at 50 hpf and found that *MZgper-/-* embryos had reduced heart rate compared to wildtype (Fig 2F, mean difference in heart rate between wildtype and mutant -30.80 ± 7.07 bpm). These results demonstrate that GPER is required for normal basal heart rate in embryos and strongly suggest that endogenous estrogens influence heart rate via GPER.

Nuclear estrogen receptor mutants exhibit normal embryonic heart rate

Whether GPER acts as an autonomous estrogen receptor *in vivo* is controversial. Previous reports suggest that GPER activity might require interaction with nuclear estrogen receptors at the membrane or that estrogens activate GPER indirectly, by binding to nuclear receptors in the cytosol that then activate downstream proteins, including GPER [15, 29]. To determine whether nuclear estrogen receptors influence heart rate, we generated zebrafish with loss-of-function mutations in each nuclear estrogen receptor gene: *esr1* (ERα), *esr2a* (ERβ1) and *esr2b* (ERβ2) (S2–S4 Figs). All mutant embryos were viable and grossly normal, allowing us to measure heart rate (S2–S4 Figs). To test whether estradiol increases heart rate via nuclear estrogen receptors, we exposed 49 hpf *esr1*$^{-/-}$, *esr2a*$^{-/-}$ and *esr2b*$^{-/-}$ embryos to estradiol, G1 or vehicle for one hour and assayed heart rate. Following estradiol exposure, heart rate was increased in all mutants compared to vehicle control (Fig 3A, mean difference in heart rate between estradiol and vehicle 25.04 ± 9.83 bpm for *esr1*$^{-/-}$, 37.23 ± 13.27 bpm for *esr2a*$^{-/-}$, 32.48 ± 3.33 bpm for *esr2b*$^{-/-}$; mean difference in heart rate between G1 and vehicle 23.26 ± 2.68 for *esr1*$^{-/-}$, 31.63 ± 13.54 for *esr2a*$^{-/-}$, 38.38 ± 18.50 for *esr2b*$^{-/-}$), similar to what we observed when wildtype embryos were exposed to estradiol (Fig 1). These results demonstrate that nuclear estrogen receptors are not necessary for estradiol-dependent increase in heart rate.

To test whether endogenous estrogens regulate heart rate via nuclear estrogen receptors, we bred heterozygous fish to generate embryos homozygous for mutations in either *esr1*, *esr2a* or

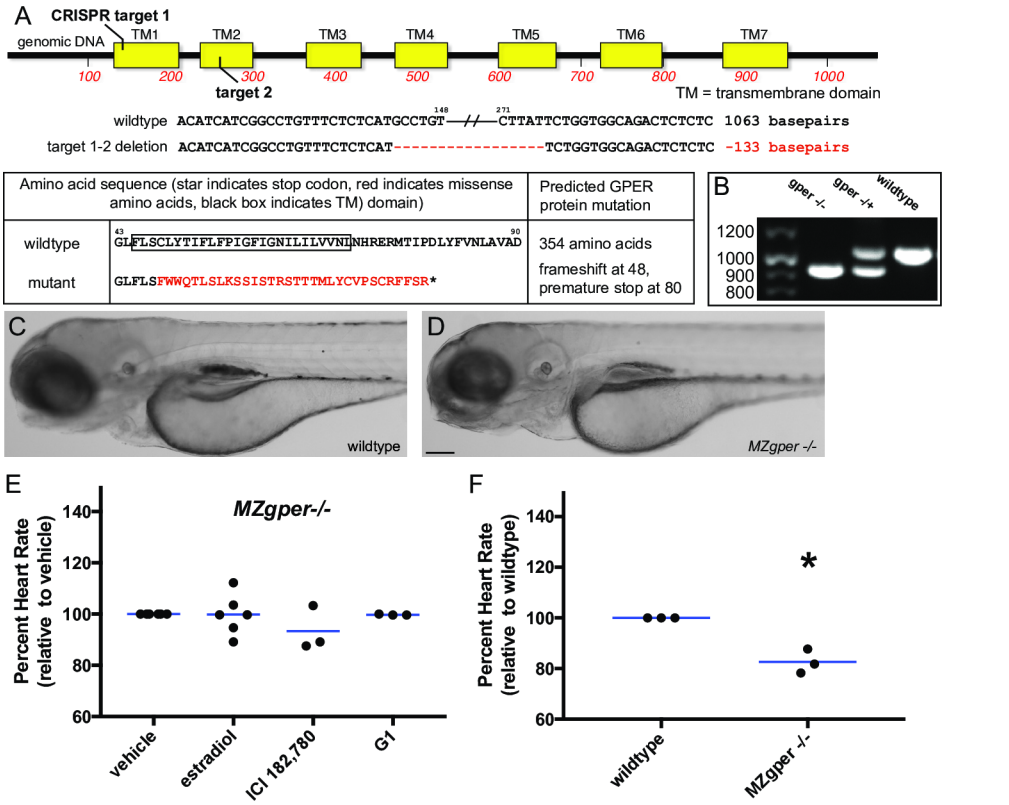

Fig 2. Abnormal heart rate in *gper* mutant zebrafish. (A) Genomic DNA of *gper*^{uab102} zebrafish contains a 133 basepair deletion in the *gper* coding region between CRISPR guide RNA targets 1 and 2, resulting in a premature stop codon in the GPER protein. Red dashes indicate DNA deletions, mutated amino acids are shown in red. **(B)** Genomic DNA was harvested from individual embryos, *gper* was PCR amplified and separated on an agarose gel to identify deletion mutations. **(C-D)** 3 day post fertilization wildtype and maternal zygotic *gper*^{uab102} homozygous larvae (*MZgper-/-*) exhibit similar gross morphology. Images are lateral views, anterior to the left, dorsal to the top. Scale bar, 500 μm. **(E)** Neither estradiol (ER/GPER agonist, 3.67 μM), ICI182,780 (ER antagonist/GPER agonist, 10 μM) or G1 (GPER agonist, 1 μM) changed heart rate significantly compared to vehicle (0.1% DMSO) in *MZgper-/-*, two-way ANOVA, p = 0.27. **(F)** *MZgper-/-* exhibited lower basal heart rate than age-matched wildtype embryos. *, p<0.05 compared to wildtype, paired t test. Each black circle represents the mean heart rate from a single clutch of embryos (≥ 7 embryos per clutch). Horizontal blue lines are the mean of each treatment.

https://doi.org/10.1371/journal.pgen.1007069.g002

esr2b genes and assayed heart rate in 50 hpf embryos. We observed no significant difference in basal heart rate between homozygotes, heterozygotes or wild type siblings within the same clutch (Fig 3B, mean difference in heart rate between homozygote and wildtype -4.34 ± 2.73 bpm for *esr1*, -0.46 ± 6.50 for *esr2a*, 0.63 ± 2.87 for *esr2b*; between heterozygote and wildtype -3.34 ± 2.05 for *esr1*, -0.91 ± 2.64 for *esr2a*, -0.67 ± 2.79 for *esr2b*). To test for maternal effects, we bred homozygous mutant male and females to each other to generate maternal zygotic *esr1* and *esr2a* mutant embryos (MZ*esr1*, MZ*esr2a*). Heart rate increased following acute exposure to E2 and G1 as above (S5 Fig; MZ*esr1* mean difference in heart rate E2 versus vehicle 18.69 ± 11.67, G1 versus vehicle 9.86 ± 0.57; MZ*esr2a* E2 versus vehicle 11.73 ± 1.51, G1 versus vehicle 14.20 ± 2.29). Due to a fertility defect in *esr2b* -/- females, we were unable to generate MZ*esr2b* embryos. These results suggest that nuclear estrogen receptors are not required for the establishment of normal basal heart rate in embryos.

It is possible that the mutations generated in each nuclear estrogen receptor gene do not cause loss of functional estrogen receptor proteins. To exclude this possibility and show that

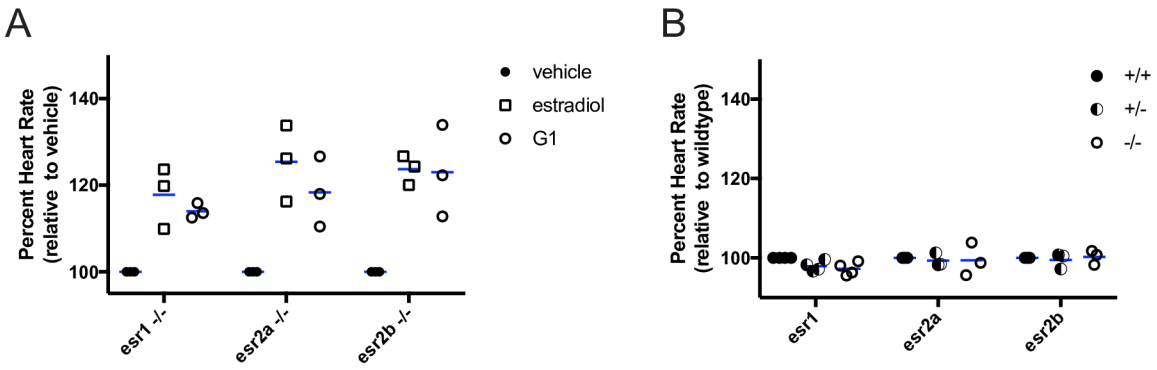

Fig 3. Normal heart rate in nuclear estrogen receptor mutants. (A) Homozygous mutant embryos at 49 hour post fertilization were incubated in water containing estradiol (ER/GPER agonist, 3.67 μM), G1 (GPER agonist, 1 μM) or vehicle (0.1% DMSO) and heart rate was measured 1 hour post treatment. Estradiol and G1 increased heart rate compared to vehicle in zebrafish with homozygous mutations in ERα (*esr1 -/-)*, ERβ1 (*esr2a -/-)*, ERβ2 (*esr2b -/-)*. For estradiol and G1 treatments, $p<0.05$ compared to vehicle within genotype, two-way ANOVA. **(B)** Basal heart rate was measured at 50 hours post fertilization in embryos reared in untreated water. Heart rate was not significantly different in homozygous mutant (-/-) embryos compared to heterozygous (-/+) and wildtype (+/+) siblings for each *esr* mutant, two-way ANOVA. Each circle or square represents the mean heart rate from a single clutch of embryos (4–8 embryos per clutch). Horizontal blue lines are the mean of each treatment or genotype.

https://doi.org/10.1371/journal.pgen.1007069.g003

esr mutants exhibit loss of functional ER proteins, we generated *esr* mutants on the *Tg(5xERE:GFP)*$^{c262/c262}$ transgenic background, where green fluorescent protein (GFP) expression occurs in cells with activated nuclear estrogen receptors [5] (referred to as 5xERE:GFP). Previous studies using whole mount *in situ* hybridization demonstrated that *esr1* is expressed in embryonic heart valves while *esr2b* is expressed in the liver [6], therefore we hypothesized that mutants would fail to upregulate GFP in tissues where the relevant receptor is normally expressed. We exposed 2–3 day post fertilization (dpf) *5xERE:GFP*, *5xERE:GFP;esr1*$^{-/-}$, *5xERE:GFP;esr2a*$^{-/-}$ and *5xERE:GFP;esr2b*$^{-/-}$ embryos to 100 ng/ml estradiol overnight and assayed fluorescence. Consistent with *esr* gene expression patterns, *5xERE:GFP;esr1*$^{-/-}$ larvae exhibited fluorescence in the liver but not in the heart (S2 Fig), whereas *5xERE:GFP;esr2b*$^{-/-}$ larvae exhibited fluorescence in the heart but not in the liver (S4 Fig). *esr2a* transcript was not detected at these embryonic and larval stages [6] and, as expected, we saw no change in fluorescence between *5xERE:GFP* and *5xERE:GFP;esr2a*$^{-/-}$ (S3 Fig). We conclude that the zebrafish nuclear estrogen receptor mutants lack estrogen receptor function.

Deleterious mutations can induce genetic compensation [30], however results from the 5xERE:GFP *esr* mutants suggest that compensatory expression of *esr* genes is not occurring. For example, it is possible that in the *esr1* mutant there is compensatory upregulation of *esr2a* and/or *esr2b* that masks a heart rate phenotype. If *esr2a* or *esr2b* were upregulated in *esr1* mutants, then we would expect to see fluorescence in the heart in *5xERE:GFP;esr1*$^{-/-}$ embryos. Instead, we observed no fluorescence in the hearts of *5xERE:GFP;esr1*$^{-/-}$ embryos (S2 Fig). Similarly, we observed no ectopic fluorescence in *5xERE:GFP;esr2b*$^{-/-}$ embryos (S4 Fig), suggesting that *esr* genes are not compensating for one another in the multiple zebrafish *esr* mutants.

To further test whether nuclear estrogen receptor signaling is influenced by GPER, we generated *gper* mutants on the *5xERE:GFP* transgenic background and asked whether estradiol exposure reduced nuclear estrogen receptor activity in mutants compared to wildtype. Following overnight exposure to estradiol, 3 dpf *5xERE:GFP* and *5xERE:GFP;MZgper-/-* larvae exhibited similar fluorescence (S6 Fig). These results demonstrate that nuclear estrogen receptor transcriptional activity does not require GPER and support the hypothesis that GPER acts as an autonomous estrogen receptor *in vivo*.

Evidence that GPER acts centrally to regulate heart rate

Heart rate can be modulated by cardiomyocytes in the heart, or by cells in the central nervous system. Neurons may directly innervate the heart to modulate heart rate and/or regulate the release of humoral factors, such as thyroid hormone, that bind to receptors in cardiomyocytes and regulate heart rate [31]. To determine whether GPER regulates heart rate tissue autonomously, we performed whole mount *in situ* hybridization to test whether *gper* transcripts are expressed in 50 hpf zebrafish embryo hearts. We did not detect transcript in the heart or in the vasculature. In contrast, we detected *gper* mRNA in three discrete anatomic areas of the brain: the preoptic and olfactory areas and in the ventral hypothalamus-pituitary (Fig 4A–4C). Thus, *gper* localization is consistent with the hypothesis that at 50 hpf, GPER acts in the brain, and not through cells in the heart, to regulate heart rate. At later stages of development and adulthood, it is possible that *gper* is expressed in the heart and regulates cardiac function.

Genetic evidence using *esr* mutants suggests that GPER acts independently of nuclear estrogen receptors to regulate heart rate (Fig 3). To further test the hypothesis that GPER acts as an autonomous estrogen receptor *in vivo*, we asked whether GPER and nuclear estrogen receptors are expressed in the same cells in the brain, reasoning that if GPER and nuclear estrogen receptors fail to colocalize, this would support the idea that GPER acts as an autonomous estrogen receptor *in vivo*. We exposed 1 dpf 5xERE:GFP embryos to 100 ng/ml estradiol overnight. At 48 hpf, we fixed the embryos and used two color fluorescent *in situ* hybridization to detect *gfp* and *gper* transcripts simultaneously. Since all three nuclear estrogen receptor genes activate the 5xERE:GFP transgene, detecting *gfp* allows us to monitor activity of all three estrogen receptors using a single RNA probe. In the olfactory and preoptic areas, we found no colocalization between *gfp* and *gper* (Fig 4D and 4E). In the ventral hypothalamus, we found a cluster of cells at the midline expressing *gper* but not *gfp*. Surrounding this region of *gper*-positive cells was a bilaterally symmetric 'U'-shaped labeling pattern of cells expressing both *gper* and *gfp* (Fig 4F). These results demonstrate that GPER and nuclear estrogen receptors are expressed in unique and overlapping cells in the brain, supporting the hypothesis that GPER can act independently of nuclear estrogen receptors *in vivo*.

gper expression in the pituitary

At 2 dpf, the ventral hypothalamus and pituitary are contiguous, therefore *gper* could be expressed in both locations. To determine whether *gper* is expressed in the pituitary, we performed whole-mount two color fluorescent *in situ* hybridization to detect *gper* and pituitary cell markers: thyroid stimulating hormone (*tshb)*, expressed in thyrotropes in the middle zone of the pituitary, and proopiomelanocortin (*pomca)*, expressed in corticotropes and melanotropes in the anterior and posterior zones of the pituitary, respectively [32, 33]. We identified a subpopulation of *tshb*-positive cells that also expressed *gper* (Fig 4G), suggesting that GPER functions in thyrotropic pituitary cells. In the anterior zone, we identified cells expressing both *gper* and *pomca* (Fig 4H). In contrast, we detected no *gper* transcript in cells in the posterior zone of the pituitary (Fig 4H"). We conclude that *gper* is expressed in the embryonic pituitary, including in thyrotropes and corticotropes.

GPER regulates estradiol and thyroid hormone levels

The pituitary regulates systemic levels of many hormones, such as gonadotropins and thyroid hormones. Because *gper* is expressed in the pituitary, we wondered whether GPER is required for pituitary development or function. To test this idea, we measured levels of hormones regulated by the pituitary: the principle endogenous estrogens estrone (E1), estradiol (E2) and estriol (E3), and thyroid hormone triiodothyronine (T3). Pituitary gonadotropins stimulate

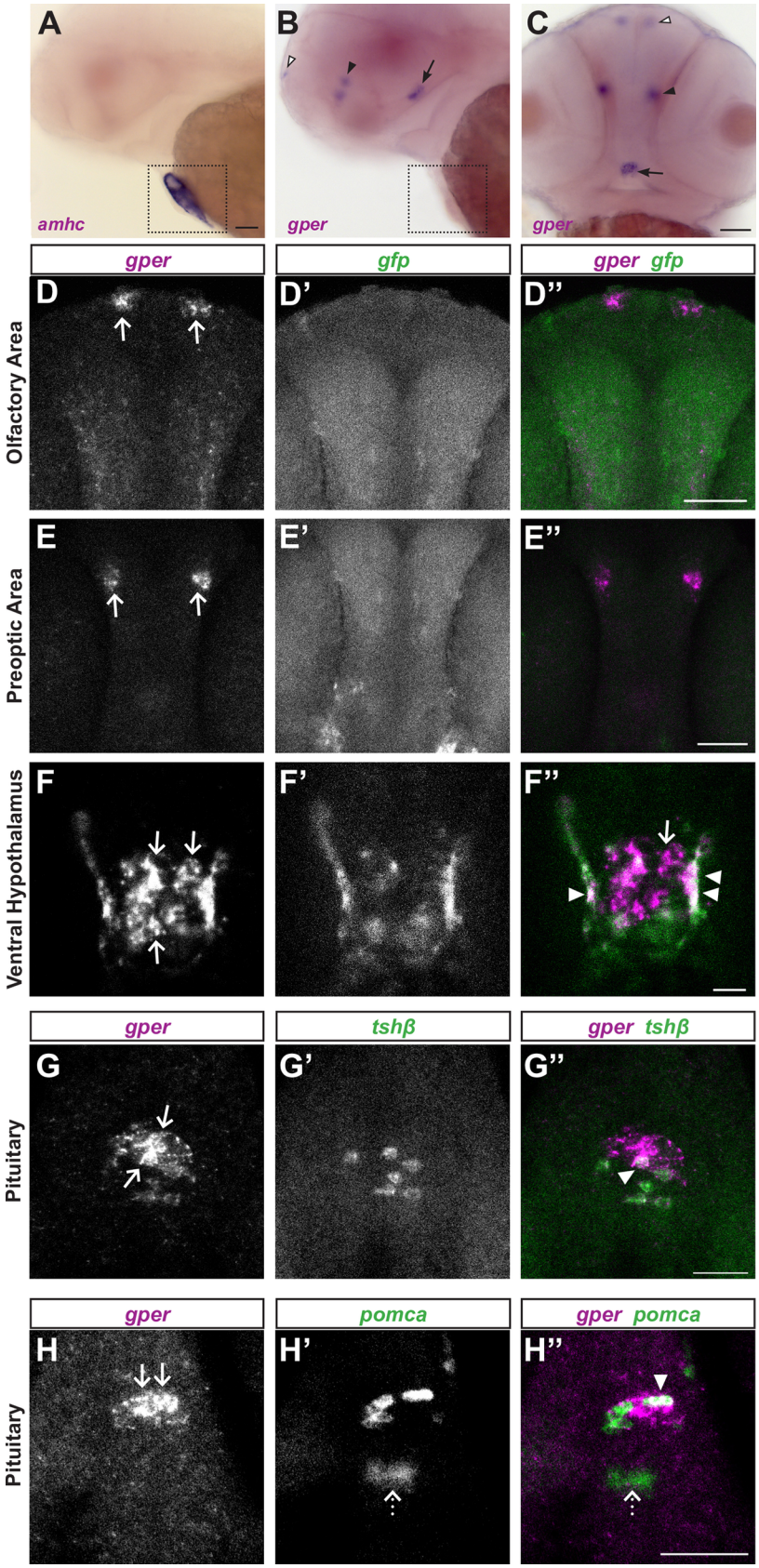
A
amhc
B
gper
C
gper
gper
gfp
gper gfp
Olfactory Area
D
D'
D''
Preoptic Area
E
E'
E''
Ventral Hypothalamus
F
F'
F''
gper
tshβ
gper tshβ
Pituitary
G
G'
G''
gper
pomca
gper pomca
Pituitary
H
H'
H''

Fig 4. *gper* expression in the brain and pituitary. (A-C) Whole mount colorimetric *in situ* hybridization was performed on wildtype embryos at 50 hours post fertilization (hpf). **(A)** *amhc* (alpha-myosin heavy chain) antisense RNA labels atrial myocardial cells in the heart (boxed). **(B, C)** *gper* antisense RNA labels a bilaterally symmetric cluster of cells in the olfactory area (white arrowheads) and preoptic area (black arrowhead) and a medial cluster of cells in the ventral hypothalamus (arrows). No label was detected in the heart. Lateral views with anterior to the left (A,B), ventral view with anterior to the top (C), scale bars = 100 μm. **(D-F)** Double fluorescent *in situ* hybridization performed on 48 hpf *Tg(5xERE:GFP)c262* embryos following overnight exposure to 100 ng/ml estradiol. *gfp* marks cells with active nuclear estrogen receptors. Confocal images of selected Z-slices (0.975 μm) show that *gper* is expressed in the olfactory area (D) and preoptic area (E) in cells lacking *gfp* (D", E", scale bars = 50 μm). In the ventral hypothalamus (F), *gper* is expressed in a medial cluster of cells lacking *gfp* (arrows, F, F"), whereas *gper* is expressed together with *gfp* more laterally (arrowheads, F", scale bar = 10 μm). **(G-H)** Double fluorescent *in situ* hybridization performed on 48 hpf wild-type embryos. Confocal images of selected Z-slices (0.975 μm) show that *gper* is expressed in the middle zone of the pituitary (G, arrows), together with *tshb*-positive thyrotropes (G", arrowhead). *gper* is expressed in the anterior zone (H, arrows) together with *pomca*-positive corticotropes (H", arrowhead). *gper* was not detected in the posterior zone of the pituitary, marked by a distinct population of *pomca*-positive cells (dotted arrows, H', H"). Scale bars = 50 μm, dorsal views, anterior to the top. In merged images, *gper* is magenta, *gfp* is green and areas of colocalization are white.

https://doi.org/10.1371/journal.pgen.1007069.g004

the ovary to synthesize estrogens, which are released into systemic circulation and thought to be deposited into oocyte yolks and absorbed by the embryo [34]. Thyrotrope cells in the pituitary regulate levels of thyroid hormone T3, which increases heart rate in mammals [35–45]. Using a new mass spectrometry assay to measure circulating estrogen levels in zebrafish blood plasma, we found that adult MZ*gper* female zebrafish had lower levels of E2 and E1 compared to wild-type females (Table 1, wild-type female mean 32 ng/ml E2, 487 pg/ml E1; MZ*gper* female <25 pg/ml E2 and E1, below limit of detection; E3 below limit of detection in all samples). Among wild-type fish, we observed reduced levels of E1 and E2 in males compared to females (Table 1), consistent with the idea that females have higher circulating levels of estrogens than males and supporting the validity of the assay. Using an enzyme linked immunosorbent assay to detect T3, we observed that MZ*gper* embryos showed a 50% reduction in total T3 levels compared to wild-type embryos (Fig 5A). We conclude that *gper* mutants have reduced levels of E1, E2 and T3, consistent with an abnormal pituitary.

Table 1. Estrogen levels in adult *gper* mutants.

Genotype	Sex	Age (days)	SL (mm)	E1 (pg/ml)	E2 (ng/ml)	E3 (pg/ml)
wt	♂	414	29.91	134	BLD	BLD
	♂	414	29.20	131	1.10	BLD
	♂	414	30.38	BLD	BLD	BLD
wt	♀	414	30.43	383	15.60	BLD
	♀	414	29.86	439	77.00	BLD
	♀	414	30.95	639	3.57	BLD
MZ*gper*	♂	379	30.65	209	0.227	BLD
	♂	379	30.12	553	0.392	BLD
	♂	379	30.11	BLD	0.525	BLD
MZ*gper*	♀	379	27.18	BLD	BLD	BLD
	♀	379	26.97	BLD	BLD	BLD
	♀	379	30.19	BLD	BLD	BLD

Levels of estrone (E1), estradiol (E2) and estriol (E3) were measured from blood plasma in adult wild type (wt) and maternal zygotic gpermutants (MZgper). Each row represents levels from an individual fish. BLD, below limit of detection (25 pg/ml). SL, standard length in millimeters.

https://doi.org/10.1371/journal.pgen.1007069.t001

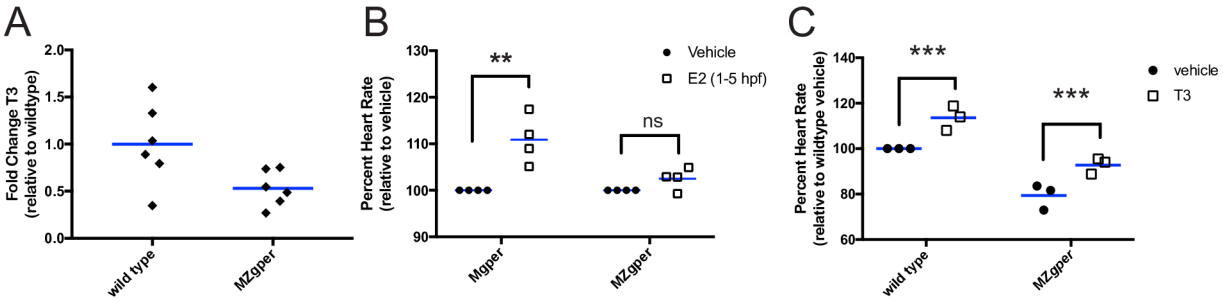

Fig 5. Triiodothyronine is reduced in *gper* mutants and rescues *gper* mutant heart rate phenotype. (A) Triiodothyronine (T3) levels are reduced in maternal zygotic *gper*^{uab102} mutants (MZ*gper*) compared to wild type. Each black diamond represents mean results of sample duplicates from 50 pooled embryos at 49 hours post fertilization (hpf). p<0.05, two-tailed t test MZ*gper* vs wild type. **(B)** Maternal *gper* mutant embryos (M*gper*, reduced maternal estrogens) and MZ*gper* embryos (reduced maternal estrogens and lacking functional *gper*) were exposed to estradiol (1 μM E2) or vehicle from 1–5 hpf to rescue maternal deposition of E2. Embryos were washed and reared in untreated water. Heart rate was assayed at 50 hpf. E2 exposure rescued heart rate in M*gper* but not in MZ*gper* embryos. ** p<0.01 compared to vehicle, paired t test; ns, not significant. **(C)** T3 (5 nM) exposure at 49 hpf increases heart rate at 50 hpf in wild type and MZ*gper* embryos compared to vehicle (0.1% methanol). ***p<0.0005 compared to vehicle within genotype, two-way ANOVA. Each circle or square represents the mean heart rate from a single clutch of embryos (6–12 embryos per clutch). Horizontal blue lines are the mean of each treatment or genotype.

https://doi.org/10.1371/journal.pgen.1007069.g005

T3 acts downstream of GPER to increase heart rate

To determine the order in which E2 and T3 act in the GPER signaling pathway, we performed pharmacologic rescue experiments. We depleted maternal estrogens in the presence or absence of *gper* by generating maternal (M*gper*) or maternal zygotic (MZ*gper*) *gper* mutant embryos and asked whether exogenous E2 or T3 could rescue the heart rate phenotype. M*gper* embryos, derived from breeding *gper*-/- females with wild-type males, have reduced deposition of maternal estrogens but express wild-type *gper*. MZ*gper* embryos, derived from breeding *gper* -/- males with *gper* -/- females, have reduced deposition of maternal estrogens and lack functional *gper*. Both M*gper* and MZ*gper* embryos have reduced basal heart rate compared to wild type (S7 Fig; difference between wild type and M*gper* -24.5 ± 3.42 bpm, between wild type and MZ*gper* -25.4 ± 1.62). We found that E2 increased heart rate only when wild-type *gper* was present, in M*gper* but not in MZ*gper* embryos (Fig 5B; M*gper* difference between E2 and vehicle 17.94 ± 7.05, MZ*gper* difference between E2 and vehicle 3.44 ± 3.35). In contrast, T3 increased heart rate in the absence of both E2 and GPER, in MZ*gper* embryos (Fig 5C, mean difference in MZ*gper* heart rate between T3 and vehicle 23.60 ± 4.98 bpm). Therefore, we conclude that T3 acts downstream of E2 and GPER.

To confirm that T3 increases heart rate in zebrafish as it does in mammals, we exposed wild-type embryos to T3 and found a mean 13% increase in heart rate compared to embryos exposed to vehicle (Fig 5C; mean difference in heart rate 22.86 ± 3.43 bpm). We also confirmed that heart rate increased in M*gper* embryos following G1 exposure (S7 Fig; mean difference between G1 and vehicle 28.63 ± 8.09), demonstrating that M*gper* embryos express zygotic wild-type *gper*.

We conclude that adult *gper* mutant females have lower levels of circulating estrogens than wild-type females and consequently deposit less estrogens into embryos. Our results support a model whereby GPER, likely acting in the pituitary, regulates estrogen levels in adult females, allowing sufficient maternal deposition of estrogens into oocytes. As embryos develop, the maternally deposited estrogens activate GPER, leading to increased T3 levels and proper heart rate (Fig 6).

Discussion

GPER regulates heart rate independently of nuclear estrogen receptors

Here we provide evidence that estrogens signal through a non-canonical estrogen receptor, the G protein-coupled estrogen receptor (GPER), to regulate heart rate in zebrafish embryos by

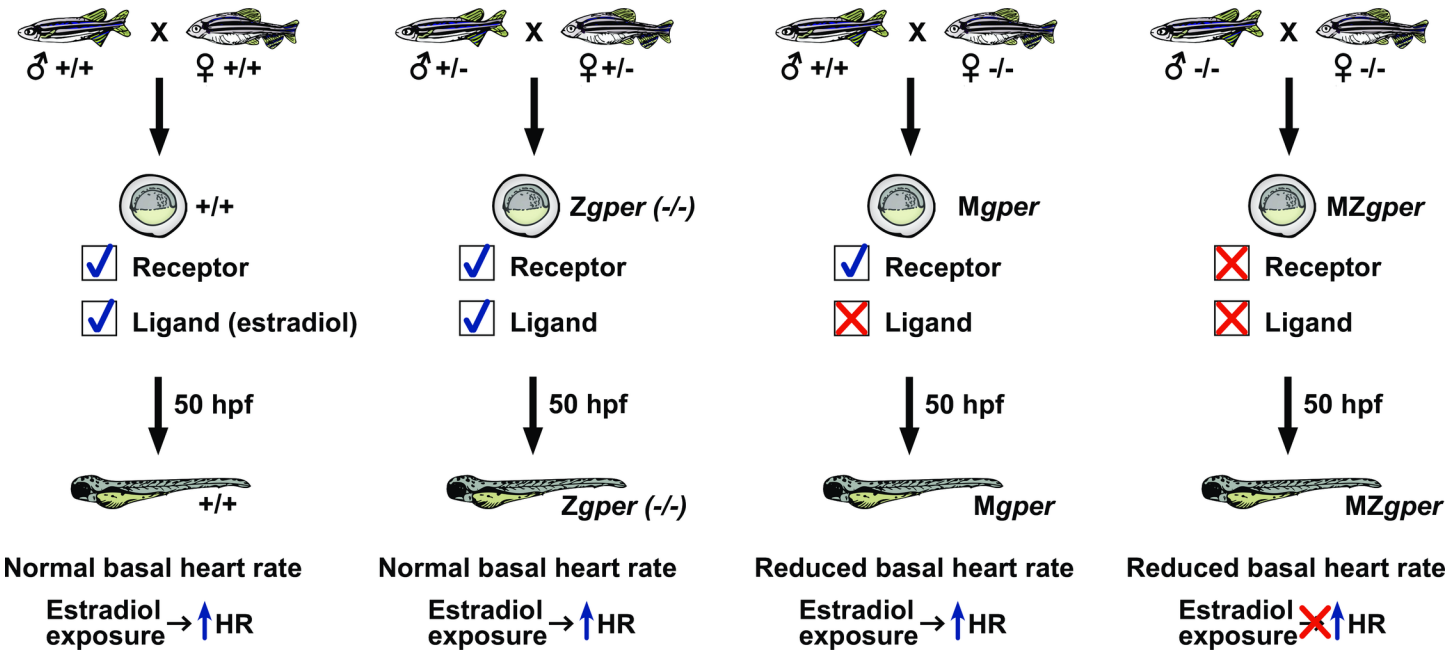

Fig 6. Model for GPER regulation of maternal estrogens and embryonic heart rate. The G protein-coupled estrogen receptor (GPER) can be maternally deposited into embryos or transcribed by embryos. A GPER ligand, estradiol, is maternally deposited in embryos but not synthesized by embryos through 50 hours post fertilization (hpf). Wildtype (+/+) and zygotic *gper* homozygous mutant embryos (*Zgper*) exhibit normal heart rate and normal response to estradiol because of maternally deposited ligand and maternally deposited receptor. Adult *gper* -/- females have reduced circulating levels of estradiol. Thus, the progeny of *gper* -/- females (M*gper* and MZ*gper* embryos) have reduced basal heart rate at 50 hpf because of the reduction of maternal estradiol. M*gper* embryos exposed to exogenous estradiol exhibit increased heart rate due to the presence of zygotic GPER (maternal *gper* is not required in the presence of zygotic *gper*). In contrast, MZ*gper* embryos exposed to estradiol exhibit no increase in heart rate because MZ*gper* embryos lack both maternal and zygotic *gper*.

https://doi.org/10.1371/journal.pgen.1007069.g006

regulating levels of maternally deposited estrogens and by altering levels of thyroid hormone T3 in embryos. Our results also support the hypothesis that GPER acts as an autonomous estrogen receptor *in vivo*. Previous reports using cultured cells demonstrated that fluorescently labeled or isotopic estradiol specifically binds membranes from cells expressing GPER [8, 9]. Additionally, estradiol exposure increased cyclic AMP and calcium levels in HEK293 and COS7 cells in a GPER-dependent manner [8, 9], while estradiol exposure increased phosphoinositide 3-kinase activity in SKBR3 breast cancer cell line in a GPER-dependent manner [8]. However, because these studies utilized cells that either express artificially high levels of GPER or are tumorigenic, the findings do not address whether GPER acts as an estrogen receptor *in vivo* under normal physiologic conditions. Our genetic and pharmacologic results strongly suggest that GPER is an estrogen receptor *in vivo*. If estradiol was binding to ERα or ERβ, and these receptors activated GPER, then we would expect to see no increase in heart rate in *esr1*, *esr2a* or *esr2b* mutants following exposure to estradiol. Instead, all *esr* mutants responded normally to estradiol and G1 exposure (Fig 3, S5 Fig), suggesting that ER and GPER signaling pathways are distinct in this context. Consistent with these results, we found *gper* transcript expressed in cells in the brain that lack nuclear estrogen receptor activity (Fig 4), further supporting the hypothesis that GPER responds to estrogens independently of nuclear estrogen receptors *in vivo*. Studying the influence of estrogens on heart rate in zebrafish embryos is a powerful *in vivo* system where GPER activity is dissociated from classical nuclear estrogen receptor signaling.

Maternal estrogens regulate embryonic heart rate

Between 2 and 5 dpf, zebrafish heart rate normally increases [46, 47]. Our results support the hypothesis that endogenous estradiol regulates this increase in heart rate. The finding that M*gper* and MZ*gper* embryos have lower basal heart rate compared to wild type implicates endogenous estradiol. Additionally, a recent HPLC analysis of endogenous estradiol concentration in zebrafish embryos found that estradiol concentrations increased from 137 pg/embryo at 48 hpf to 170 pg/embryo at 72 hpf [48]. However, whether this increase in embryonic estradiol is due to increased synthesis by embryos or increased release of estrogens from the yolk is not known.

Our genetic and mass spectrometry results support the hypothesis that at 48 hpf, maternally derived estrogens are required for normal heart rate. Data from M*gper* embryos suggests that, in the absence of maternal deposition of estrogens, basal heart rate is reduced. Since wild-type *gper* is present in M*gper* embryos, the reduced basal heart rate in M*gper* embryos is due to reduced maternal deposition of estrogens (leading to reduced activation of wild-type GPER) and not due to mutant *gper* (Fig 6). We cannot exclude the possibility that reduced maternal estrogen levels indirectly caused reduced GPER activity in embryos in an estrogen-independent manner, though this seems unlikely.

The identity of the physiologic estrogen (or estrogens) that regulates heart rate is not known. Our mass spectrometry results implicate E2, the most potent and abundant endogenous estrogen in humans [49] and many vertebrate species. However, E1 levels were also reduced in *gper* mutant females compared to wild-type females (Table 1), thus E1 may also contribute to regulation of heart rate. Many other endogenous estrogens exist, such as 27-hydroxycholesterol and estetrol [50, 51], and it will be interesting to see to what degree they are present in embryos, regulate embryonic heart rate and activate GPER.

GPER regulates thyroid hormone levels to influence heart rate

There are several mechanisms by which GPER activity in the brain could regulate heart rate, for example by modulating sympathetic and parasympathetic nerve activity or by regulating the release of humoral factors, such as thyroid hormone. Expression of *gper* transcript in thyrotropic cells in the pituitary (Fig 4) and decreased levels of total T3 in *gper* mutants (Fig 5) support the latter hypothesis. There are three primary mechanisms by which GPER could promote the increase of total T3: 1) by increasing levels of thyroid stimulating hormone, leading to release of thyroxine (T4) from the thyroid, which is then converted to T3, 2) by increasing the conversion of T4 to T3, or 3) by blocking the conversion of T3 into inactive metabolites, such as 3,5-Diiodo-L-thyronine (T2) and reverse T3 (RT3; 3,3'5'-triiodothyronine). *gper* expression in *tshb*-positive cells in the pituitary supports the first hypothesis. In humans, thyroid stimulating hormone is thought to be required for the differentiation of the thyroid [52]. Curiously, zebrafish mutant embryos that lack thyrotrope progenitor cells and *tsh* gene expression still produce thyroid follicle cells and T4 [53]. This suggests that thyrotropes may not be required to produce T3, however total T3 was not measured in this study. It is possible that the localized production of T4 is sufficient to stimulate thyroid development, while total T3 is reduced. In support of this, a majority of the cartilage in the pharynx is missing in thyrotrope deficient zebrafish [53], which suggests that even though the thyroid begins to differentiate, tissues adjacent to the thyroid do not, presumably due to reduced total T4 in circulation. While TSH signaling may not be required for the development of the thyroid, it may be required for secondary functions, including proper regulation of heart rate.

We cannot exclude the possibility that GPER activity leads to increased expression or activity of deiodinase enzymes that convert T4 to T3, or that GPER activity reduces the expression

or activity of enzymes that metabolize T3. All four deiodinases genes (*dio1*, *dio2*, *dio3a* and *dio3b*) are expressed in zebrafish as early as 24 hpf [54] and are therefore available to convert thyroid hormones at 48 hpf, when we observe changes in heart rate. Interestingly, at 24 hpf *dio2*, the enzyme that converts T4 to T3, is expressed in the pituitary [55] in addition to its expression in the thyroid. *dio3a*, which inactivates T3 by conversion to RT3 and T2, is also expressed in the brain and thyroid at 24 hpf [55]. Previous work suggests that GPER influences neurotransmitter release and cAMP levels [56]. cAMP was shown to increase deiodinase activity in the brain leading to increased T3 levels [57–59]. Therefore, GPER activity could trigger neuronal activity that leads to increased activity of deiodinases and increased production of T3, independently of TSH, to regulate heart rate [31].

A new connection between estrogen and thyroid hormone signaling

More generally, it is not known to what extent estrogens influence thyroid hormone signaling. Our work suggests that endogenous estrogens influence T3 levels. Previous work suggests that environmental estrogens may also influence thyroid hormone signaling. Exposure to the plasticizer diethylhexyl phthalate (DEHP) increased total T3 levels in zebrafish larvae and upregulated thyroid signaling genes thyroglobulin (*tg*), transthyretin (*ttr*), and *dio2* [60]. DEHP exhibits estrogen-like activity, although the receptor by which it acts has not been determined. DEHP can inhibit tamoxifen-induced apoptosis and also induce cell proliferation in GPER positive MCF-7 cells, but not in GPER negative MDA-MB-231 cells [61], suggesting that DEHP can activate GPER. One possibility is that DEHP increases T3 levels in zebrafish larvae via GPER activation. Similarly, chronic exposure to perfluorooctanesulphonic acid (PFOS), a surfactant that enhances the effects of estradiol [62], increased total T3 levels in juvenile zebrafish and upregulated thyroid signaling genes including thyroid hormone receptor β, the sodium/iodide symporter *slc5a5*, *dio1* and *dio2* [63]. We speculate that like estradiol, the environmental endocrine disruptors DEHP and PFOS modulate T3 levels by activating GPER. This raises the important consideration that diverse environmental estrogens could alter thyroid signaling and thus cardiac function.

GPER function beyond embryonic development

While our results illuminate GPER signaling in the context of embryonic heart rate, it is not clear to what extent GPER influences heart rate at later stages of development. At larval, juvenile and adult stages it is difficult to assess heart rate without immobilizing or anesthetizing zebrafish, manipulations that themselves may influence heart rate. In adult mice with mutations in GPER, there was no significant difference in basal heart rate between mutant and wild type of either sex [16, 17, 64]. It is possible that GPER regulates heart rate in embryos but not in adults. Additionally, heart rate in GPER mutant mice was assayed using general anesthesia, which is known to depress heart rate compared to conscious mice [65]. Anesthesia may mask the effect of GPER on basal heart rate that we observe in conscious animals. We also cannot exclude the possibility that the effects of GPER on heart rate are specific for zebrafish.

The fact that adult *gper* mutant females have reduced circulating E2 and E1 suggests that *gper* mutants will exhibit additional phenotypes in juvenile and adult stages of life. It is possible that female *gper* mutants have reduced fertility or become infertile at an earlier age compared to wild type, phenotypes that the current study was not powered to detect. Additionally, reduced estrogen levels may indicate deficits in locomotor activity, mating behavior or aggression, behaviors known to be influenced by estrogens [66–71].

Considering that GPER deficient zebrafish embryos have reduced T3 levels, it will be interesting to examine whether this deficiency exists at later developmental stages and whether

GPER mutant adults have growth and metabolic defects consistent with reduced total T3. In MZ*gper* embryos, we observed no gross morphological detects up to 2 dpf, while mutant adults are viable and fertile. Zebrafish mutants with ~70–90% reduced total T3 levels due to genetic ablation of *dio2* exhibit delayed swim bladder inflation, altered locomotor activity through 7 dpf, delayed fertility, reduced number of eggs, and reduction in viable fertilized eggs [72]. In GPER deficient fish, the reduction in T3 levels is less drastic and we anticipate seeing less severe phenotypes as a result of the more modest decrease in T3.

Using zebrafish estrogen receptor mutants to study developmental effects of exposure to environmental endocrine disruptors

The zebrafish estrogen receptor mutants we developed enable experiments to rapidly and conclusively identify the causative estrogen receptor associated with any estrogen signaling phenotype, as demonstrated with the estradiol-dependent increase in heart rate reported here. This has significant implications for studies of estrogenic environmental endocrine disruptors, which are frequently tested on zebrafish to identify effects on embryonic development, organ formation and function [73]. Zebrafish estrogen receptor mutants can now be used to determine whether such effects are specific for estrogen receptors and to identify the precise receptor target. Our results also establish a need to consider the impact on cardiac function when considering the toxicity of estrogenic environmental endocrine disruptors.

Materials and methods

Zebrafish

Zebrafish were raised at 28.5˚C on a 14-h light, 10-h dark cycle in the UAB Zebrafish Research Facility in a recirculating water system (Aquaneering, Inc., San Diego, CA). Wildtype zebrafish were AB strain [74] and all mutant and transgenic lines were generated on the AB strain. To visualize nuclear estrogen receptor activity, transgenic line *Tg(5xERE:GFP)*$^{c262/c262}$ was used for all studies unless otherwise mentioned [5]. All procedures were approved by the UAB Institutional Animal Care and Use Committee.

Embryo collection

Embryos were collected during 10 minute intervals to ensure precise developmental timing within a group. Embryos were placed in Petri dishes containing E3B (60X E3B: 17.2g NaCl, 0.76g KCl, 2.9g $CaCl_2$-$2H_2O$, 2.39g $MgSO_4$ dissolved in 1 liter Milli-Q water; diluted to 1X in 9 liter Milli-Q water plus 100 μL 0.02% methylene blue) and placed in an incubator at 28.5˚C on a 14-h light, 10-h dark cycle. At 24 hours post fertilization (hpf), embryos were incubated in E3B containing 200 μM 1-phenyl 2-thiourea (PTU) to inhibit pigment production [74]. Between 24 and 48 hpf, embryos were manually dechorionated and randomly divided into control and experimental treatment groups in 60mm Petri dishes and kept at 28.5˚C until 49 hpf.

Embryo treatments

At 49 hpf, embryos were incubated in E3B with estrogen receptor modulator(s) at 28.5˚C for 1 hour. Estrogen receptor modulator treatments consisted of: 3.67 μM E2 (17β-estradiol; Sigma E8875, purity ≥ 98%), 10 μM ICI182,780 (fulvestrant; Sigma I4409, purity >98%), 1 μM G1 (Azano AZ0001301, purity ≥ 98%), 1 μM G36 (Azano, AZ-0001303, purity ≥ 98%), 1 μM progesterone (Sigma P0130, purity ≥ 99%), 5 nM 3,3′,5-Triiodo-L-thyronine (T3; Sigma T2877, purity ≥ 95%), vehicle (0.1% dimethylsulfoxide (DMSO), Fisher D128-500; purity ≥ 99.9% or

0.1% methanol, Fisher A411-4). All chemical stocks were made in 100% DMSO at 1000x and diluted in E3B embryo media to final concentration at the time of treatment, except for T3 which was made in 100% methanol for chemical stocks but was diluted in E3B media as above. Exposure concentrations were chosen based on previous evidence of efficacy. 3.67 μM E2 and 10 μM ICI were previously shown to be effective at activating and inhibiting nuclear estrogen receptor activity in zebrafish embryos [5, 6]. The doses of G1 and G36 were selected based on reports that chronic exposure to G1 elicits concentration-dependent effects on gross morphology and gene expression, which are blocked by G36 [28, 75] (note that since we exposed zebrafish to G1 and G36 for only 1 hour, we did not observe defects in gross morphology). We chose 1 μM progesterone because it is non-toxic following 1 hour exposure and because previous studies have demonstrated that <1 μM concentrations are effective at regulating progestin-dependent gene expression in zebrafish embryos and larvae [76–79]. The T3 concentration used was previously shown to be effective at inducing thyroid hormone-dependent gene expression and premature differentiation of pectoral fins in zebrafish [54, 80]. For rescue experiments (ICI182,780 + G36), final DMSO concentration was 0.2%. There was no difference in heart rate between embryos incubated in 0.1% or 0.2% DMSO (not shown). All vehicle controls shown in figures are 0.1% DMSO, except where indicated.

Measurement of heart rates

All embryos were reared at 28.5˚C and heart rate was measured at room temperature. Following one hour incubation in treatment compounds at 28.5˚C, heart rate (beats per minute, bpm) was calculated by counting the number of heart beats in fifteen seconds and multiplying that number by four. Prior to measurements, each dish was removed from the incubator and placed under the microscope light for 4 minutes at room temperature, allowing embryos to acclimate to the light and eliminate any effect of the startle response. At the time of heart rate measurement, water temperature was 25˚C (assayed with Fisher Scientific digital thermometer with stainless steel probe, catalogue number 15-077-9D). Control groups were counted first and last to ensure that the overall heart rate did not increase during the duration of counting due to natural increases in heart rate during development. All heart rates were measured on a Zeiss Stemi 2000 dissecting microscope with a halogen transmitted light base (Carl Zeiss Microimaging, Thornwood, NJ). Absolute heart rates in wildtype, untreated (or vehicle control treated) embryos at 48–50 hpf were frequently 140–150 bpm, consistent with previous studies [46, 81–83]. However, there is variability in heart rate, despite controlling for conditions such as developmental stage and water temperature, due to factors we do not yet understand. For example, on some days, wildtype heart rate was approximately 130 bpm (see S1 Table). However, the change in heart rate between treated and untreated embryos, or between wildtype and mutant embryos, was always consistent, irrespective of the absolute heart rate values recorded on the day we performed the experiment (see S1 Table for absolute heart rate data). Therefore, we report both mean difference in heart rate between groups (not normalized) and fold difference in heart rate compared to control (normalized). We performed a rigorous statistical analysis on the non-normalized data to determine whether differences in heart rate were due to clutch and day variability and found that differences in heart rate were due to the effects of treatment or genotype (see Experimental Design and Data Analysis).

Generation of guide RNA and Cas9 mRNA

Plasmids pT7-gRNA and pT3TS-nCas9n were obtained from Addgene (numbers 46759, 46757) [27]. pT7-gRNA was digested simultaneously with BsmBI, BglII and SalI for one hour at 37 °C followed by one hour at 55 °C. To generate *esr2a*, *esr2b* and *gper* gRNAs,

Table 2. Target site sequences for *gper*, *esr1*, *esr2b* and *esr2a* oligonucleotides.

Gene	CRISPR target[a]	Oligo 1	Oligo 2
esr1	GTCCTCTCAGCAGGCAGCCGTGG	ATTTAGGTGACACTATA	GTTTTAGAGCTAGAAATAGCAAG
esr2a	GGAGAGGATGAGTTGAAGATGGG	TAGGAGAGGATGAGTTGAAGAT	AAACATCTTCAACTCATCCTCT
esr2b	GGCGGGCAGTGCAGAGAGTGAGG	TAGGCGGGCAGTGCAGAGAGTG	AAACCACTCTCTGCACTGCCCG
gper target 1	GGCTGTGGCAGATCTTATTCTGG	TAGGCTGTGGCAGATCTTATTC	AAACGAATAAGATCTGCCACAG
gper target 2	GGAAAAGGAAAATGGTGTACAGG	TAGGAAAAGGAAAATGGTGTAC	AAACGTACACCATTTTCCTTTT

[a]PAM nucleotides are underlined

https://doi.org/10.1371/journal.pgen.1007069.t002

oligonucleotides containing target site sequences (Table 2) were synthesized by Invitrogen. Oligos were hybridized to each other using NEBuffer3 restriction enzyme buffer (New England Biolabs) to generate double stranded target DNA and annealed into digested pT7-gRNA using Quick T4 DNA Ligase (New England Biolabs) as previously described [27]. Guide RNAs were synthesized using the MegaShortScript T7 Kit (Life Technologies) using the relevant modified pT7-gRNA vector linearized with BamHI as a template. Guide RNA was purified using the RNA clean & concentrator kit (Zymo Research). To generate *esr1* guide RNA, target-specific oligonucleotides containing the SP6 (5'-ATTTAGGTGACACTATA) promoter sequence, a 20 basepair target site without the PAM, and a complementary region were annealed to a constant oligonucleotide encoding the reverse-complement of the tracrRNA tail as described [84]. This oligo was used as a template for in vitro transcription using the MegaShortScript Sp6 Kit (LifeTechnologies). To generate *Cas9* mRNA, the pT3TS-nCas9n plasmid was linearized with XbaI and transcribed using the mMessage mMachine T3 kit (Life Technologies) and purified using RNA clean & concentrator kit (Zymo Research). RNA concentration was quantified using a Nanodrop spectrophotometer (Nanodrop ND-1000, ThermoFisher).

Embryo injections

One-cell-stage embryos were injected using glass needles pulled on a Sutter Instruments Fleming/Brown Micropipette Puller, model P-97 and a regulated air-pressure micro-injector (Harvard Apparatus, NY, PL1–90). Each embryo was injected with a 1 nl solution of 150 ng/μl of Cas9 mRNA, 50 ng/μl of gRNA and 0.1% phenol red. Mixtures were injected into the yolk of each embryo. Approximately 100 injected embryos per gRNA were raised to adulthood and crossed to wild-type fish (either AB or *Tg5xERE:GFP*^{c262}) to generate F1 embryos. F1 offspring with heritable mutations were sequenced to identify loss of function mutations.

Genomic DNA isolation

Individual embryos or tail biopsies from individual adults were placed in 100 μL ELB (10 mM Tris pH 8.3, 50 mM KCl, 0.3% Tween 20) with 1 μL proteinase K (800 U/ml, NEB) in 96 well plates, one sample per well. Samples were incubated at 55˚C for 2 hours (embryos) or 8 hours (tail clips) to extract genomic DNA. To inactivate Proteinase K, plates were incubated at 98˚C for 10 minutes and stored at -20˚C.

High resolution melt curve analysis

PCR and melting curve analysis was performed as described [85]. PCR reactions contained 1 μl of LC Green Plus Melting Dye (BioFire Diagnostics), 1 μl of Ex Taq Buffer, 0.8 μl of dNTP Mixture (2.5 mM each), 1 μl of each primer (5 μM), 0.05 μl of Ex Taq (Takara Bio Inc), 1 μl of

genomic DNA, and water up to 10 μl. PCR was performed in a Bio-Rad C1000 Touch thermal cycler, using black/white 96 well plates (Bio-Rad HSP9665). PCR reaction protocol was 98˚C for 1 min, then 34 cycles of 98˚C for 10 sec, 60˚C for 20 sec, and 72˚C for 20 sec, followed by 72˚C for 1 min. After the final step, the plate was heated to 95˚C for 20 sec and then rapidly cooled to 4˚C. Melting curves were generated with either a LightScanner HR 96 (Idaho Technology) over a 70–95˚C range and analyzed with LightScanner Instrument and Analysis Software (V. 2.0.0.1331, Idaho Technology, Inc, Salt Lake City, UT), or with a Bio-Rad CFX96 Real-Time System over a 70–95˚C range and analyzed with Bio-Rad CFX Manager 3.1 software. All mutations were confirmed by TA cloning and sequencing.

Live imaging

Live zebrafish embryos and larvae were visualized using a Nikon MULTIZOOM AZ100 equipped with epi-fluorescence and an Andor Clara digital camera unless otherwise noted. To validate mutants with 5xERE reporter activity, larvae were treated overnight with 100 ng/mL estradiol beginning at 2–3 dpf. Following overnight treatment, larvae were washed in E3B, anesthetized with 0.04% tricaine and imaged in Petri dish containing E3B. For S1H–S1K Fig, larvae were mounted in bridged coverslips in E3B with 0.04% tricaine [74]. Images were captured on a Zeiss Axio Observer.Z1 fluorescent microscope equipped with an Axio HRm camera and Zen Blue 2011 software (Carl Zeiss Microscopy, Oberkochen, Germany). Adjustments, cropping and layout were performed using Photoshop CC and InDesign CC (Adobe Systems Inc., San Jose, CA).

RNA in situ hybridization

For synthesis of RNA probes, full-length *gper* open reading frame was amplified by PCR from genomic DNA extracted from 3 dpf larvae (*gper* coding region is within a single exon and therefore the open reading frame sequence is identical in genomic and cDNA) using primers 5'-ATGGAGGAGCAGACTACCAATGTG-3' and 5'-CTACACCTCAGACTCACTCCTGA CAG-3'.

For *tshb* probe, a 252bp product was amplified by PCR from cDNA (prepared from total RNA from 5 dpf AB larvae using RETROscript reverse transcription kit (ThermoFisher Scientific) with oligo(dT) primers) using primers 5' GAGTTGGTGGGTCCTCGTTT 3' and 5' TGCTTGGGCGTAGTTGTTCT 3'. Each product was then TA cloned into pCR2.1 vector (Invitrogen). *amhc* and *gfp* probes were used as described [5, 86]. All clones were verified by sequencing. Digoxigenin-labeled antisense RNA and FITC-labeled antisense RNA were transcribed using T7 and T3 polymerase, respectively, as previously described [5].

Colorimetric whole-mount *in situ* hybridization was performed on zebrafish embryos and larvae as described previously, using 5% dextran in the hybridization buffer [87, 88]. Following colorimetric *in situ* hybridization, embryos were sequentially cleared in glycerol (25%, 50%, 75% in phosphate buffered saline), mounted in 4% low-melting temperature agarose, and imaged using a Zeiss Axio Observer.Z1 microscope with Zeiss Axio MRc5 camera and Zen Blue 2011 software. Fluorescent *in situ* hybridization (FISH) was performed as previously described [88] with the following modifications: After rehydration, Proteinase K treatment was extended to 35 minutes. Following hybridization, embryos were washed in 2xSSC prior to being placed in PBT. Embryos were blocked in 2% Roche blocking reagent in 100 mM Maleic acid, 150 mM NaCl, pH 7.5 [89]. For double labeling, following development of anti-DIG-POD antibody, reaction was inactivated in 100 mM glycine pH 2 for 10 minutes then incubated in anti-FITC antibody. Following florescent *in situ* hybridization, embryos were cleared

in 50% glycerol, mounted on a bridged coverslip and imaged using a Nikon A1/R scanning confocal microscope with Nikon Advanced Elements software.

Measuring T3 levels in embryos

T3 levels were measured using enzyme-linked immunosorbent assay as previously described [90], with minor modifications, using T3 ELISA Kit (IBL America IB19107). Briefly, 50 embryos were pooled in 50 μl of PBS and pulsed sonicated intermittently for 5 minutess, alternating 5 second sonication and 5 seconds on ice, then vortexed intermittently for 10 minutes, alternating 30 seconds vortexing and 30 seconds on ice. Samples where then centrifuged for 10 minutes at 15,000g at 4˚C. Supernatant was collected and diluted 1:8 in PBS. 50 μl was used per reaction in accordance with the manufacturer's instructions. Each sample was tested in duplicate and the mean of duplicates were compared statistically.

Measuring estrogen levels in adult plasma

Plasma from adult zebrafish was collected as described [91] with the following modifications. Zebrafish were anesthetized in 0.04 mg/mL tricaine then patted dry. Standard length [92] was measured with digital calipers. The caudal fin was completely severed with a razor blade and discarded, then each fish was transferred into a perforated 0.5 mL microcentrifuge tube placed inside a 1.5 mL microcentrifuge tube containing 10 μL heparin (5 mg/mL in water; Sigma-Aldrich #H3393). Fish were centrifuged (1000 rpm, 5 minutes, 4˚C), then the tail was cut above the previous incision and centrifuged with the same parameters. Whole blood collected in the 1.5 mL tube was then centrifuged (14000 rpm, 15 minutes, 4˚C) to isolate plasma (supernatant). Plasma was stored at -80˚C until mass spectrometry analysis.

Prior to mass spectrometry, plasma samples were initially subjected to a liquid-liquid extraction using hexane:ethyl acetate, followed by derivatization with dansyl chloride and then the final solid-phase extraction before analysis. Estrone-d_4, Estradiol-d_5, and Estriol-d_3 (Toronto Research Chemicals Inc., North York, Ontario, Canada) were used as internal standards. E1, E2, E3 and respective internal standards were eluted from a C18 column (XSelect HSS T3, 2.1x75mm, 2.5μm, Waters Corporation, Milford, MA) using mobile phase gradient where mobile phase A consisted of 0.1% formic acid in water and mobile phase B consisted of 0.1% formic acid in acetonitrile:isopropanol. Analytes were detected in positive ion mode using multiple reaction monitoring (Sciex Qtrap 6500+ with IonDrive TurboV Source, Sciex, Foster City, CA): E1, 504.1→171.1 m/z; E2, 506.1→171.1 m/z; E3, 522.1→171.1 m/z; E1-d_4, 508.1→171.1 m/z; E2-d_5, 511.1→171.1 m/z; and E3-d_3, 525.1→171.1 m/z. The dynamic range of the assay was 25 to 2500 picograms/mL for each of the target analytes using 5μL of plasma.

Experimental design and data analysis

Heart rate assays were conducted in separate experiments. Each experiment included comparing groups (treated vs untreated or mutant vs wildtype) using at least 3 embryos per group with all embryos from the same clutch. All experiments were replicated at least 3 times ($n \geq 3$) using different clutches. This is essentially a complete block design with clutch as block. Mean heart rate of individual embryos from a clutch was used for comparing treatment groups (or mutant groups) within experiments using two-way ANOVA controlling for clutch effect. The overall treatment effect (or the genotype effect in some experiments) was tested using F test. If it was significant, Dunnett's test was then used to compare each treatment group with the vehicle group or mutant group with the wildtype group. For some individual pairs of comparisons, paired t test was used. Significance level is 0.05. All the analyses were conducted using R (version 3.0.2). Graphs were produced using GraphPad Prism 7.0c software.

Supporting information

S1 Fig. Zygotic *gper*$^{uab102/uab102}$ mutant embryos are sensitive to estradiol. (A) Genomic DNA sequence of zebrafish *gper* open reading frame, contained in a single exon. Highlighted nucleotides are deleted in *uab102*. **(B)** Chromatogram of *uab102* genomic DNA sequence. 133 basepair deletion occurred in between highlighted thymine (T) nucleotides. **(C)** Zygotic homozygous *gper* mutant embryos were incubated in water containing estradiol (ER/GPER agonist, 3.67 μM) or vehicle control (0.1% DMSO) at 49 hours post fertilization and heart rates were measured 1 hour post treatment. *, $p<0.05$ compared to vehicle, paired t test. Each black circle represents the mean heart rate from a single clutch of embryos ($\geq$ 6 embryos per clutch). Clutches in the same treatment group were assayed on different days. Horizontal blue lines are the mean of each treatment.
(PDF)

S2 Fig. Generation and validation of *esr1* mutant zebrafish. (A) Genomic DNA of *esr1*^{uab118} zebrafish contains a 4 basepair deletion in the *esr1* coding region, resulting in a premature stop codon in the Esr1 (ERα) protein. Nucleotide deletions are shown as red dashes, amino acid mutations are in red. Map indicates site of frameshift mutation and premature stop codon (AF-1, activating function 1 domain; DBD, DNA binding domain; LBD, ligand binding domain; AF-2, activating function 2 domain). **(B)** High resolution melting curve analysis was used to distinguish mutants from wildtype. Curves represents DNA amplified from a wildtype AB (black) or *esr1*^{uab118} mutant zebrafish (cyan). **(C)** Strategy for validating zebrafish estrogen receptor mutants using transgenic 5xERE:GFP zebrafish. Mutants were generated on a transgenic background where estrogen receptor (ER) transcriptional activity is marked by green fluorescent protein (GFP) expression. Following exposure to estradiol, loss-of-function mutants should exhibit reduced fluorescence in cells expressing *esr1*. **(D-K)** 2-day post fertilization embryos were exposed to 367 nM (100 ng/mL) estradiol, live fluorescent images (D, F, H, J) and corresponding brightfield images (E, G, I, K) were taken at 3 d. *5xERE:GFP*^{c262}; *esr1*^{uab118} homozygous larvae (*esr1* -/-) exhibit normal morphology, but lack fluorescence in heart valves, wheres heterozygotes (*esr1* -/+) exhibit fluorescent heart valves. High magnification images of the heart are shown in H-K. Arrows indicate heart valves, arrow head indicates liver. Images are lateral views, anterior to the left, dorsal to the top. Scale bars, 500 μm (D-G), 100 μm (H-K).
(PDF)

S3 Fig. Generation of *esr2a* mutant zebrafish. (A) Genomic DNA of *esr2a*^{uab134} zebrafish contains an 2 basepair deletion (red dashes) in the *esr2a* coding region, resulting in a premature stop codon in the Esr2a (ERβ1) protein. Amino acid mutations are in red. Map indicates frameshift mutation and premature stop codon in the Esr2a protein. AF-1, activating function 1 domain; DBD, DNA binding domain; LBD, ligand binding domain; AF-2, activating function 2 domain. **(B)** High resolution melting curve analysis was used to distinguish mutants from wildtype. Curves represent DNA amplified from a wildtype AB (black) or *esr2a*^{uab134} mutant zebrafish (cyan). **(C-F)** *5xERE:GFP*^{c262} *and 5xERE:GFP*^{c262}*;esr2a*^{uab134} *(esr2a* -/-) 3-day post fertilization (d) larvae were exposed to 367 nM (100 ng/mL) estradiol. Live fluorescent images (C, E) and corresponding brightfield images (D, F) were captured at 4 d. *esr2a* -/- larvae exhibit normal morphology and fluorescence, consistent with data demonstrating that *esr2a* is not expressed during these developmental stages. Arrows indicate heart valves, arrow head indicates liver. Images are lateral views, anterior to the left, dorsal to the top. Scale bar, 500 μm.
(PDF)

S4 Fig. Generation and validation of *esr2b* mutant zebrafish. (A) Genomic DNA of *esr2b*^{uab127} zebrafish contains a 5 basepair deletion (red) in the *esr2b* coding region, resulting in a premature stop codon in the Esr2b (ERβ2) protein. Amino acid mutations are in red. Map indicates frameshift mutation and premature stop codon in the Esr2b protein. AF-1, activating function 1 domain; DBD, DNA binding domain; LBD, ligand binding domain; AF-2, activating function 2 domain. **(B)** High resolution melting curve analysis was used to distinguish mutants from wildtype. Curves represents DNA amplified from a wildtype AB (black) or *esr2b*^{uab127} mutant zebrafish (cyan). **(C-F)** *5xERE:GFP*^{c262}*;esr2b*^{uab127} 3-day post fertilization (d) larvae were exposed to 367 nM (100 ng/mL) estradiol. Live fluorescent images (C, E) and corresponding brightfield images (D, F) were captured at 4 d. *5xERE:GFP*^{c262}*;esr2b*^{uab127} homozygous larvae (*esr2b* -/-) exhibit normal morphology, but lack fluorescence in the liver. Arrows indicate heart valves, arrow head indicates liver. Images are lateral views, anterior to the left, dorsal to the top. Scale bar = 100 μm.
(PDF)

S5 Fig. Maternal zygotic *esr* mutant embryos are sensitive to estradiol and G1. Maternal zygotic homozygous *esr1* and *esr2a* mutant embryos (MZ*esr1*, MZ*esr2a*) were incubated in water containing estradiol (ER/GPER agonist, 3.67 μM), G1 (GPER agonist, 1 μM) or vehicle control (0.1% DMSO) at 49 hours post fertilization and heart rates were measured 1 hour post treatment. Each circle or square represents the mean heart rate from a single independent clutch of embryos (9–13 embryos per clutch). Horizontal lines are the mean of each treatment.
(PDF)

S6 Fig. Nuclear estrogen receptor transcriptional activity is normal in *gper* mutant zebrafish. (A-H) Maternal zygotic *gper*^{uab102} homozygous larvae on the *5xERE:GFP*^{c262} transgenic background (MZ*gper*) were exposed to 367 nM (100 ng/mL) estradiol at 2-days post fertilization (2 d). Fluorescence (A, C, E, G) and corresponding brightfield images (B, D, F, H) were taken at 3 d. Fluorescence in the heart valves (arrows) and liver (arrow heads) is similar between MZ*gper* and wild type. C, D, G, H, High magnification images of heart. Images are lateral views, anterior to the left, dorsal to the top. Scale bars, 500 μm (C-F), 100 μm (G-J).
(PDF)

S7 Fig. Maternal effects of *gper* mutation. (A) Basal heart rate was measured at 51 hours post fertilization (hpf) in embryos reared in untreated water. Maternal zygotic homozygous *gper* mutants (MZ*gper*), produced by breeding homozygous mutant females with homozygous males, and maternal *gper* mutants (M*gper*), produced by breeding homozygous mutant females with wild-type males, had reduced heart rate compared to wild type. *** $p<0.001$ compared to wild type, two-way ANOVA. **(B)** M*gper* embryos at 49 hpf were incubated in water containing G1 (GPER agonist, 1 μM) or vehicle (0.1% DMSO) and heart rate was measured 1 hour post treatment. G1 increased heart rate compared to vehicle, $p<0.05$, paired t test. Each circle represents the mean heart rate from a single clutch of embryos (6–12 embryos per clutch). Horizontal blue lines are the mean of each treatment or genotype.
(PDF)

S1 Table. Raw heart rate data for each figure.
(XLSX)

Acknowledgments

We thank J.L. King for technical assistance, C.M. Crowder for help with blood plasma collection, E.P. Acosta for advice on mass spectrometry, M.A. Miller for critical comments on the manuscript, and S.C. Farmer and the staff of the UAB zebrafish facility for animal care.

Author Contributions

Conceptualization: Shannon N. Romano, Daniel A. Gorelick.

Data curation: Daniel A. Gorelick.

Formal analysis: Shannon N. Romano, Hailey E. Edwards, Jaclyn Paige Souder, Kevin J. Ryan, Xiangqin Cui, Daniel A. Gorelick.

Funding acquisition: Daniel A. Gorelick.

Investigation: Shannon N. Romano, Hailey E. Edwards, Jaclyn Paige Souder, Daniel A. Gorelick.

Methodology: Shannon N. Romano, Hailey E. Edwards, Jaclyn Paige Souder, Kevin J. Ryan, Xiangqin Cui, Daniel A. Gorelick.

Project administration: Daniel A. Gorelick.

Supervision: Daniel A. Gorelick.

Writing – original draft: Shannon N. Romano, Hailey E. Edwards, Jaclyn Paige Souder, Kevin J. Ryan, Xiangqin Cui, Daniel A. Gorelick.

Writing – review & editing: Shannon N. Romano, Hailey E. Edwards, Jaclyn Paige Souder, Kevin J. Ryan, Xiangqin Cui, Daniel A. Gorelick.

References

1. Staudt D, Stainier D. Uncovering the Molecular and Cellular Mechanisms of Heart Development Using the Zebrafish. Annual Review of Genetics. 2012; 46(1):397–418. https://doi.org/10.1146/annurev-genet-110711-155646 PMID: 22974299
2. Liu X, Zhu P, Sham KW, Yuen JM, Xie C, Zhang Y, et al. Identification of a membrane estrogen receptor in zebrafish with homology to mammalian GPER and its high expression in early germ cells of the testis. Biology of reproduction. 2009; 80(6):1253–61. Epub 2009/02/21. https://doi.org/10.1095/biolreprod.108.070250 PMID: 19228597.
3. Menuet A, Pellegrini E, Anglade I, Blaise O, Laudet V, Kah O, et al. Molecular characterization of three estrogen receptor forms in zebrafish: binding characteristics, transactivation properties, and tissue distributions. Biology of reproduction. 2002; 66(6):1881–92. PMID: 12021076.
4. Thomas P, Alyea R, Pang Y, Peyton C, Dong J, Berg AH. Conserved estrogen binding and signaling functions of the G protein-coupled estrogen receptor 1 (GPER) in mammals and fish. Steroids. 2010; 75(8–9):595–602. https://doi.org/10.1016/j.steroids.2009.11.005 PMID: 19931550
5. Gorelick DA, Halpern ME. Visualization of Estrogen Receptor Transcriptional Activation in Zebrafish. Endocrinology. 2011; 152(7):2690–703. https://doi.org/10.1210/en.2010-1257 PMID: 21540282
6. Gorelick DA, Iwanowicz LR, Hung AL, Blazer VS, Halpern ME. Transgenic zebrafish reveal tissue-specific differences in estrogen signaling in response to environmental water samples. Environmental health perspectives. 2014; 122(4):356–62. https://doi.org/10.1289/ehp.1307329 PMID: 24425189; PubMed Central PMCID: PMC3984228.
7. Evans R. A transcriptional basis for physiology. Nat Med. 2004; 10(10):1022–6. Epub 2004/10/02. https://doi.org/10.1038/nm1004-1022 PMID: 15459694.
8. Revankar CM, Cimino DF, Sklar LA, Arterburn JB, Prossnitz ER. A Transmembrane Intracellular Estrogen Receptor Mediates Rapid Cell Signaling. Science. 2005; 307(5715):1625–30. https://doi.org/10.1126/science.1106943 PMID: 15705806
9. Thomas P, Pang Y, Filardo EJ, Dong J. Identity of an estrogen membrane receptor coupled to a G protein in human breast cancer cells. Endocrinology. 2005; 146(2):624–32. Epub 2004/11/13. https://doi.org/10.1210/en.2004-1064 PMID: 15539556.
10. Navarro CE, Abdul Saeed S, Murdock C, Martinez-Fuentes AJ, Arora KK, Krsmanovic LZ, et al. Regulation of cyclic adenosine 3',5'-monophosphate signaling and pulsatile neurosecretion by Gi-coupled plasma membrane estrogen receptors in immortalized gonadotropin-releasing hormone neurons. Mol Endocrinol. 2003; 17(9):1792–804. Epub 2003/06/24. https://doi.org/10.1210/me.2003-0040 PMID: 12819297.

11. Wu Q, Chambliss K, Lee WR, Yuhanna IS, Mineo C, Shaul PW. Point mutations in the ERalpha Galphai binding domain segregate nonnuclear from nuclear receptor function. Mol Endocrinol. 2013; 27(1):2–11. Epub 2012/12/18. https://doi.org/10.1210/me.2011-1378 PMID: 23242705; PubMed Central PMCID: PMCPmc3545213.
12. Kumar P, Wu Q, Chambliss KL, Yuhanna IS, Mumby SM, Mineo C, et al. Direct interactions with G alpha i and G betagamma mediate nongenomic signaling by estrogen receptor alpha. Mol Endocrinol. 2007; 21(6):1370–80. Epub 2007/04/05. https://doi.org/10.1210/me.2006-0360 PMID: 17405905.
13. Watson CS, Jeng YJ, Hu G, Wozniak A, Bulayeva N, Guptarak J. Estrogen- and xenoestrogen-induced ERK signaling in pituitary tumor cells involves estrogen receptor-alpha interactions with G protein-alphai and caveolin I. Steroids. 2012; 77(5):424–32. Epub 2012/01/11. https://doi.org/10.1016/j.steroids.2011.12.025 PMID: 22230296; PubMed Central PMCID: PMCPMC3304022.
14. Vivacqua A, Lappano R, De Marco P, Sisci D, Aquila S, De Amicis F, et al. G protein-coupled receptor 30 expression is up-regulated by EGF and TGF alpha in estrogen receptor alpha-positive cancer cells. Mol Endocrinol. 2009; 23(11):1815–26. Epub 2009/09/15. https://doi.org/10.1210/me.2009-0120 PMID: 19749156.
15. Levin ER. G Protein-Coupled Receptor 30: Estrogen Receptor or Collaborator? Endocrinology. 2009; 150(4):1563–5. https://doi.org/10.1210/en.2008-1759 PMID: 19307418
16. Delbeck M, Golz S, Vonk R, Janssen W, Hucho T, Isensee J, et al. Impaired left-ventricular cardiac function in male GPR30-deficient mice. Molecular medicine reports. 2011; 4(1):37–40. Epub 2011/04/05. https://doi.org/10.3892/mmr.2010.402 PMID: 21461560.
17. Martensson UE, Salehi SA, Windahl S, Gomez MF, Sward K, Daszkiewicz-Nilsson J, et al. Deletion of the G protein-coupled receptor 30 impairs glucose tolerance, reduces bone growth, increases blood pressure, and eliminates estradiol-stimulated insulin release in female mice. Endocrinology. 2009; 150(2):687–98. Epub 2008/10/11. https://doi.org/10.1210/en.2008-0623 PMID: 18845638.
18. Haas E, Bhattacharya I, Brailoiu E, Damjanovic M, Brailoiu GC, Gao X, et al. Regulatory role of G protein-coupled estrogen receptor for vascular function and obesity. Circ Res. 2009; 104(3):288–91. https://doi.org/10.1161/CIRCRESAHA.108.190892 PMID: 19179659; PubMed Central PMCID: PMC2782532.
19. Meyer MR, Fredette NC, Howard TA, Hu C, Ramesh C, Daniel C, et al. G protein-coupled estrogen receptor protects from atherosclerosis. Sci Rep. 2014; 4:7564. Epub 2014/12/24. https://doi.org/10.1038/srep07564 PMID: 25532911; PubMed Central PMCID: PMCPMC4274506.
20. Takahashi T. Juvenile hermaphroditism in the zebrafish, Brachydanio rerio. Bull Fac Fish Hokkaido Univ. 1977; 28(2):57–65.
21. vom Saal FS. Variation in phenotype due to random intrauterine positioning of male and female fetuses in rodents. Journal of reproduction and fertility. 1981; 62(2):633–50. Epub 1981/07/01. PMID: 7252935.
22. vom Saal FS. Sexual differentiation in litter-bearing mammals: influence of sex of adjacent fetuses in utero. Journal of animal science. 1989; 67(7):1824–40. Epub 1989/07/01. PMID: 2670873.
23. Pang Y, Dong J, Thomas P. Estrogen signaling characteristics of Atlantic croaker G protein-coupled receptor 30 (GPR30) and evidence it is involved in maintenance of oocyte meiotic arrest. Endocrinology. 2008; 149(7):3410–26. https://doi.org/10.1210/en.2007-1663 PMID: 18420744; PubMed Central PMCID: PMCPMC2453078.
24. Robertson JF. ICI 182,780 (Fulvestrant)—the first oestrogen receptor down-regulator—current clinical data. British journal of cancer. 2001; 85 Suppl 2:11–4. https://doi.org/10.1054/bjoc.2001.1982 PMID: 11900210.
25. Dennis MK, Field AS, Burai R, Ramesh C, Petrie WK, Bologa CG, et al. Identification of a GPER/GPR30 antagonist with improved estrogen receptor counterselectivity. The Journal of steroid biochemistry and molecular biology. 2011; 127(3–5):358–66. Epub 2011/07/26. https://doi.org/10.1016/j.jsbmb.2011.07.002 PMID: 21782022; PubMed Central PMCID: PMCPMC3220788.
26. Bologa CG, Revankar CM, Young SM, Edwards BS, Arterburn JB, Kiselyov AS, et al. Virtual and biomolecular screening converge on a selective agonist for GPR30. Nat Chem Biol. 2006; 2(4):207–12. https://doi.org/10.1038/nchembio775 PMID: 16520733.
27. Jao LE, Wente SR, Chen W. Efficient multiplex biallelic zebrafish genome editing using a CRISPR nuclease system. Proc Natl Acad Sci U S A. 2013; 110(34):13904–9. Epub 2013/08/07. https://doi.org/10.1073/pnas.1308335110 PMID: 23918387; PubMed Central PMCID: PMCPMC3752207.
28. Jayasinghe BS, Volz DC. Aberrant ligand-induced activation of G protein-coupled estrogen receptor 1 (GPER) results in developmental malformations during vertebrate embryogenesis. Toxicol Sci. 2012; 125(1):262–73. Epub 2011/10/11. https://doi.org/10.1093/toxsci/kfr269 PMID: 21984484.
29. Langer G, Bader B, Meoli L, Isensee J, Delbeck M, Noppinger PR, et al. A critical review of fundamental controversies in the field of GPR30 research. Steroids. 2010; 75(8–9):603–10. Epub 2009/12/26. https://doi.org/10.1016/j.steroids.2009.12.006 PMID: 20034504.

30. Rossi A, Kontarakis Z, Gerri C, Nolte H, Holper S, Kruger M, et al. Genetic compensation induced by deleterious mutations but not gene knockdowns. Nature. 2015; 524(7564):230–3. Epub 2015/07/15. https://doi.org/10.1038/nature14580 PMID: 26168398.

31. Klein I, Ojamaa K. Thyroid hormone and the cardiovascular system. The New England journal of medicine. 2001; 344(7):501–9. Epub 2001/02/15. https://doi.org/10.1056/NEJM200102153440707 PMID: 11172193.

32. Herzog W, Sonntag C, Walderich B, Odenthal J, Maischein HM, Hammerschmidt M. Genetic analysis of adenohypophysis formation in zebrafish. Mol Endocrinol. 2004; 18(5):1185–95. https://doi.org/10.1210/me.2003-0376 PMID: 14752054.

33. Herzog W, Zeng X, Lele Z, Sonntag C, Ting JW, Chang CY, et al. Adenohypophysis formation in the zebrafish and its dependence on sonic hedgehog. Dev Biol. 2003; 254(1):36–49. Epub 2003/02/28. PMID: 12606280.

34. Carroll KJ, Esain V, Garnaas MK, Cortes M, Dovey MC, Nissim S, et al. Estrogen defines the dorsal-ventral limit of VEGF regulation to specify the location of the hemogenic endothelial niche. Dev Cell. 2014; 29(4):437–53. https://doi.org/10.1016/j.devcel.2014.04.012 PMID: 24871948.

35. Macchia PE, Takeuchi Y, Kawai T, Cua K, Gauthier K, Chassande O, et al. Increased sensitivity to thyroid hormone in mice with complete deficiency of thyroid hormone receptor alpha. Proc Natl Acad Sci U S A. 2001; 98(1):349–54. https://doi.org/10.1073/pnas.011306998 PMID: 11120878; PubMed Central PMCID: PMCPMC14593.

36. Wikstrom L, Johansson C, Salto C, Barlow C, Campos Barros A, Baas F, et al. Abnormal heart rate and body temperature in mice lacking thyroid hormone receptor alpha 1. EMBO J. 1998; 17(2):455–61. https://doi.org/10.1093/emboj/17.2.455 PMID: 9430637; PubMed Central PMCID: PMCPMC1170396.

37. Mittag J, Davis B, Vujovic M, Arner A, Vennstrom B. Adaptations of the autonomous nervous system controlling heart rate are impaired by a mutant thyroid hormone receptor-alpha1. Endocrinology. 2010; 151(5):2388–95. https://doi.org/10.1210/en.2009-1201 PMID: 20228172.

38. Carr AN, Kranias EG. Thyroid hormone regulation of calcium cycling proteins. Thyroid. 2002; 12 (6):453–7. https://doi.org/10.1089/105072502760143818 PMID: 12165106.

39. Jiang M, Xu A, Narayanan N. Thyroid hormone downregulates the expression and function of sarcoplasmic reticulum-associated CaM kinase II in the rabbit heart. American journal of physiology Heart and circulatory physiology. 2006; 291(3):H1384–94. https://doi.org/10.1152/ajpheart.00875.2005 PMID: 16617128.

40. Khoury SF, Hoit BD, Dave V, Pawloski-Dahm CM, Shao Y, Gabel M, et al. Effects of thyroid hormone on left ventricular performance and regulation of contractile and Ca(2+)-cycling proteins in the baboon. Implications for the force-frequency and relaxation-frequency relationships. Circ Res. 1996; 79(4):727–35. PMID: 8831496.

41. Shenoy R, Klein I, Ojamaa K. Differential regulation of SR calcium transporters by thyroid hormone in rat atria and ventricles. American journal of physiology Heart and circulatory physiology. 2001; 281(4): H1690–6. PMID: 11557559.

42. Katzeff HL, Powell SR, Ojamaa K. Alterations in cardiac contractility and gene expression during low-T3 syndrome: prevention with T3. The American journal of physiology. 1997; 273(5 Pt 1):E951–6. Epub 1997/12/31. PMID: 9374681.

43. Bengel FM, Nekolla SG, Ibrahim T, Weniger C, Ziegler SI, Schwaiger M. Effect of thyroid hormones on cardiac function, geometry, and oxidative metabolism assessed noninvasively by positron emission tomography and magnetic resonance imaging. J Clin Endocrinol Metab. 2000; 85(5):1822–7. Epub 2000/06/08. https://doi.org/10.1210/jcem.85.5.6520 PMID: 10843159.

44. Cacciatori V, Bellavere F, Pezzarossa A, Dellera A, Gemma ML, Thomaseth K, et al. Power spectral analysis of heart rate in hyperthyroidism. J Clin Endocrinol Metab. 1996; 81(8):2828–35. Epub 1996/08/01. https://doi.org/10.1210/jcem.81.8.8768838 PMID: 8768838.

45. Feldman T, Borow KM, Sarne DH, Neumann A, Lang RM. Myocardial mechanics in hyperthyroidism: importance of left ventricular loading conditions, heart rate and contractile state. Journal of the American College of Cardiology. 1986; 7(5):967–74. Epub 1986/05/01. PMID: 3958379.

46. De Luca E, Zaccaria GM, Hadhoud M, Rizzo G, Ponzini R, Morbiducci U, et al. ZebraBeat: a flexible platform for the analysis of the cardiac rate in zebrafish embryos. Sci Rep. 2014. https://doi.org/10.1038/srep04898 http://www.nature.com/srep/2014/140509/srep04898/abs/srep04898.html - supplementary-information.

47. de Pater E, Clijsters L, Marques SR, Lin YF, Garavito-Aguilar ZV, Yelon D, et al. Distinct phases of cardiomyocyte differentiation regulate growth of the zebrafish heart. Development. 2009; 136(10):1633–41. Epub 2009/04/28. https://doi.org/10.1242/dev.030924 PMID: 19395641; PubMed Central PMCID: PMCPmc2673760.

48. Alharthy KM, Albaqami FF, Thornton C, Corrales J, Willett KL. Mechanistic evaluation of benzo[a]pyrene's developmental toxicities mediated by reduced Cyp19a1b activity. Toxicol Sci. 2016. Epub 2016/09/17. https://doi.org/10.1093/toxsci/kfw182. PMID: 27633980.

49. Xu X, Roman JM, Issaq HJ, Keefer LK, Veenstra TD, Ziegler RG. Quantitative measurement of endogenous estrogens and estrogen metabolites in human serum by liquid chromatography-tandem mass spectrometry. Analytical chemistry. 2007; 79(20):7813–21. Epub 2007/09/13. https://doi.org/10.1021/ac070494j PMID: 17848096.

50. DuSell CD, Umetani M, Shaul PW, Mangelsdorf DJ, McDonnell DP. 27-hydroxycholesterol is an endogenous selective estrogen receptor modulator. Mol Endocrinol. 2008; 22(1):65–77. Epub 2007/09/18. https://doi.org/10.1210/me.2007-0383 PMID: 17872378; PubMed Central PMCID: PMCPmc2194632.

51. Coelingh Bennink HJ, Holinka CF, Diczfalusy E. Estetrol review: profile and potential clinical applications. Climacteric: the journal of the International Menopause Society. 2008; 11 Suppl 1:47–58. Epub 2008/06/17. https://doi.org/10.1080/13697130802073425 PMID: 18464023.

52. Parmentier M, Libert F, Maenhaut C, Lefort A, Gerard C, Perret J, et al. Molecular cloning of the thyrotropin receptor. Science. 1989; 246(4937):1620–2. PMID: 2556796.

53. Alt B, Reibe S, Feitosa NM, Elsalini OA, Wendl T, Rohr KB. Analysis of origin and growth of the thyroid gland in zebrafish. Dev Dyn. 2006; 235(7):1872–83. Epub 2006/05/09. https://doi.org/10.1002/dvdy.20831 PMID: 16680726.

54. Liu YW, Lo LJ, Chan WK. Temporal expression and T3 induction of thyroid hormone receptors alpha1 and beta1 during early embryonic and larval development in zebrafish, Danio rerio. Mol Cell Endocrinol. 2000; 159(1–2):187–95. PMID: 10687864.

55. Marelli F, Carra S, Agostini M, Cotelli F, Peeters R, Chatterjee K, et al. Patterns of thyroid hormone receptor expression in zebrafish and generation of a novel model of resistance to thyroid hormone action. Mol Cell Endocrinol. 2016; 424:102–17. Epub 2016/01/24. https://doi.org/10.1016/j.mce.2016.01.020 PMID: 26802880.

56. Waters EM, Thompson LI, Patel P, Gonzales AD, Ye HZ, Filardo EJ, et al. G-protein-coupled estrogen receptor 1 is anatomically positioned to modulate synaptic plasticity in the mouse hippocampus. The Journal of neuroscience: the official journal of the Society for Neuroscience. 2015; 35(6):2384–97. Epub 2015/02/13. https://doi.org/10.1523/jneurosci.1298-14.2015 PMID: 25673833; PubMed Central PMCID: PMCPmc4323523.

57. Kundu S, Biswas A, Roy S, De J, Pramanik M, Ray AK. Thyroid hormone homeostasis in brain: possible involvement of adrenergic phenomenon in adult rat. Neuroendocrinology. 2009; 89(2):140–51. https://doi.org/10.1159/000158715 PMID: 18818486.

58. Kundu S, Roy S, De J, Biswas A, Pramanik M, Ray AK. Maintenance of homeostasis for thyroid hormone in the adult rat brain: possible involvement of a nuclear-mediated phenomenon. Neuroendocrinology. 2007; 86(2):94–103. https://doi.org/10.1159/000107580 PMID: 17703090.

59. Safran M, Farwell AP, Leonard JL. Catalytic activity of type II iodothyronine 5'-deiodinase polypeptide is dependent upon a cyclic AMP activation factor. J Biol Chem. 1996; 271(27):16363–8. PMID: 8663169.

60. Jia PP, Ma YB, Lu CJ, Mirza Z, Zhang W, Jia YF, et al. The Effects of Disturbance on Hypothalamus-Pituitary-Thyroid (HPT) Axis in Zebrafish Larvae after Exposure to DEHP. PLoS One. 2016; 11(5):e0155762. https://doi.org/10.1371/journal.pone.0155762 PMID: 27223697; PubMed Central PMCID: PMCPMC4880181.

61. Kim IY, Han SY, Moon A. Phthalates inhibit tamoxifen-induced apoptosis in MCF-7 human breast cancer cells. J Toxicol Environ Health A. 2004; 67(23–24):2025–35. https://doi.org/10.1080/15287390490514750 PMID: 15513900.

62. Sonthithai P, Suriyo T, Thiantanawat A, Watcharasit P, Ruchirawat M, Satayavivad J. Perfluorinated chemicals, PFOS and PFOA, enhance the estrogenic effects of 17beta-estradiol in T47D human breast cancer cells. J Appl Toxicol. 2016; 36(6):790–801. https://doi.org/10.1002/jat.3210 PMID: 26234195.

63. Shi X, Liu C, Wu G, Zhou B. Waterborne exposure to PFOS causes disruption of the hypothalamus-pituitary-thyroid axis in zebrafish larvae. Chemosphere. 2009; 77(7):1010–8. https://doi.org/10.1016/j.chemosphere.2009.07.074 PMID: 19703701.

64. Meoli L, Isensee J, Zazzu V, Nabzdyk CS, Soewarto D, Witt H, et al. Sex- and age-dependent effects of Gpr30 genetic deletion on the metabolic and cardiovascular profiles of diet-induced obese mice. Gene. 2014; 540(2):210–6. Epub 2014/03/04. https://doi.org/10.1016/j.gene.2014.02.036 PMID: 24582972.

65. Janssen BJ, De Celle T, Debets JJ, Brouns AE, Callahan MF, Smith TL. Effects of anesthetics on systemic hemodynamics in mice. American journal of physiology Heart and circulatory physiology. 2004; 287(4):H1618–24. Epub 2004/05/25. https://doi.org/10.1152/ajpheart.01192.2003 PMID: 15155266.

66. Ogawa S, Lubahn DB, Korach KS, Pfaff DW. Behavioral effects of estrogen receptor gene disruption in male mice. Proc Natl Acad Sci U S A. 1997; 94(4):1476–81. PMID: 9037078.

67. Ogawa S, Lubahn DB, Korach KS, Pfaff DW. Aggressive behaviors of transgenic estrogen-receptor knockout male mice. Annals of the New York Academy of Sciences. 1996; 794:384–5. PMID: 8853623.

68. Ogawa S, Chester AE, Hewitt SC, Walker VR, Gustafsson JA, Smithies O, et al. Abolition of male sexual behaviors in mice lacking estrogen receptors alpha and beta (alpha beta ERKO). Proc Natl Acad Sci U S A. 2000; 97(26):14737–41. https://doi.org/10.1073/pnas.250473597 PMID: 11114183.

69. Musatov S, Chen W, Pfaff DW, Kaplitt MG, Ogawa S. RNAi-mediated silencing of estrogen receptor {alpha} in the ventromedial nucleus of hypothalamus abolishes female sexual behaviors. Proc Natl Acad Sci U S A. 2006; 103(27):10456–60. https://doi.org/10.1073/pnas.0603045103 PMID: 16803960.

70. Hoffman EJ, Turner KJ, Fernandez JM, Cifuentes D, Ghosh M, Ijaz S, et al. Estrogens Suppress a Behavioral Phenotype in Zebrafish Mutants of the Autism Risk Gene, CNTNAP2. Neuron. 2016; 89 (4):725–33. https://doi.org/10.1016/j.neuron.2015.12.039 PMC4766582. PMID: 26833134

71. Toda K, Okada T, Takeda K, Akira S, Saibara T, Shiraishi M, et al. Oestrogen at the neonatal stage is critical for the reproductive ability of male mice as revealed by supplementation with 17beta-oestradiol to aromatase gene (Cyp19) knockout mice. The Journal of endocrinology. 2001; 168(3):455–63. PMID: 11241177.

72. Houbrechts AM, Delarue J, Gabriels IJ, Sourbron J, Darras VM. Permanent Deiodinase Type 2 Deficiency Strongly Perturbs Zebrafish Development, Growth, and Fertility. Endocrinology. 2016; 157 (9):3668–81. https://doi.org/10.1210/en.2016-1077 PMID: 27580812.

73. McCollum CW, Ducharme NA, Bondesson M, Gustafsson JA. Developmental toxicity screening in zebrafish. Birth defects research Part C, Embryo today: reviews. 2011; 93(2):67–114. Epub 2011/06/15. https://doi.org/10.1002/bdrc.20210 PMID: 21671351.

74. Westerfield M. The Zebrafish Book. A Guide for the Laboratory Use of Zebrafish (Danio Rerio). 4th ed. Eugene, OR: University of Oregon Press; 2000.

75. Diamante G, Menjivar-Cervantes N, Leung MS, Volz DC, Schlenk D. Contribution of G protein-coupled estrogen receptor 1 (GPER) to 17beta-estradiol-induced developmental toxicity in zebrafish. Aquat Toxicol. 2017; 186:180–7. Epub 2017/03/12. https://doi.org/10.1016/j.aquatox.2017.02.024 PMID: 28284154.

76. Liang YQ, Huang GY, Ying GG, Liu SS, Jiang YX, Liu S. Progesterone and norgestrel alter transcriptional expression of genes along the hypothalamic-pituitary-thyroid axis in zebrafish embryos-larvae. Comparative biochemistry and physiology Toxicology & pharmacology: CBP. 2015; 167:101–7. Epub 2014/10/04. https://doi.org/10.1016/j.cbpc.2014.09.007 PMID: 25277675.

77. Liang YQ, Huang GY, Ying GG, Liu SS, Jiang YX, Liu S, et al. The effects of progesterone on transcriptional expression profiles of genes associated with hypothalamic-pituitary-gonadal and hypothalamic-pituitary-adrenal axes during the early development of zebrafish (Danio rerio). Chemosphere. 2015; 128:199–206. Epub 2015/02/24. https://doi.org/10.1016/j.chemosphere.2015.01.062 PMID: 25706437.

78. Rossier NM, Chew G, Zhang K, Riva F, Fent K. Activity of binary mixtures of drospirenone with progesterone and 17alpha-ethinylestradiol in vitro and in vivo. Aquat Toxicol. 2016; 174:109–22. Epub 2016/03/02. https://doi.org/10.1016/j.aquatox.2016.02.005 PMID: 26930480.

79. Zucchi S, Castiglioni S, Fent K. Progestins and antiprogestins affect gene expression in early development in zebrafish (Danio rerio) at environmental concentrations. Environ Sci Technol. 2012; 46 (9):5183–92. Epub 2012/04/06. https://doi.org/10.1021/es300231y PMID: 22475373.

80. Brown DD. The role of thyroid hormone in zebrafish and axolotl development. Proc Natl Acad Sci U S A. 1997; 94(24):13011–6. Epub 1997/12/16. PMID: 9371791; PubMed Central PMCID: PMCPMC24254.

81. Baker K, Warren KS, Yellen G, Fishman MC. Defective "pacemaker" current (Ih) in a zebrafish mutant with a slow heart rate. Proc Natl Acad Sci U S A. 1997; 94(9):4554–9. Epub 1997/04/29. PMID: 9114028; PubMed Central PMCID: PMCPmc20761.

82. Milan DJ, Peterson TA, Ruskin JN, Peterson RT, MacRae CA. Drugs That Induce Repolarization Abnormalities Cause Bradycardia in Zebrafish. Circulation. 2003; 107(10):1355–8. PMID: 12642353

83. Pelster B, Burggren WW. Disruption of hemoglobin oxygen transport does not impact oxygen-dependent physiological processes in developing embryos of zebra fish (Danio rerio). Circ Res. 1996; 79 (2):358–62. Epub 1996/08/01. PMID: 8756015.

84. Gagnon JA, Valen E, Thyme SB, Huang P, Ahkmetova L, Pauli A, et al. Efficient Mutagenesis by Cas9 Protein-Mediated Oligonucleotide Insertion and Large-Scale Assessment of Single-Guide RNAs. PLoS One. 2014; 9(5):e98186. Epub 2014/05/31. https://doi.org/10.1371/journal.pone.0098186 PMID: 24873830; PubMed Central PMCID: PMCPmc4038517.

85. Parant JM, George SA, Pryor R, Wittwer CT, Yost HJ. A rapid and efficient method of genotyping zebrafish mutants. Dev Dyn. 2009; 238(12):3168–74. Epub 2009/11/06. https://doi.org/10.1002/dvdy.22143 PMID: 19890916; PubMed Central PMCID: PMCPmc3888828.

86. Waxman JS, Keegan BR, Roberts RW, Poss KD, Yelon D. Hoxb5b acts downstream of retinoic acid signaling in the forelimb field to restrict heart field potential in zebrafish. Dev Cell. 2008; 15(6):923–34. Epub 2008/12/17. https://doi.org/10.1016/j.devcel.2008.09.009 PMID: 19081079; PubMed Central PMCID: PMCPmc2752051.

87. Thisse C, Thisse B. High-resolution in situ hybridization to whole-mount zebrafish embryos. Nature protocols. 2008; 3(1):59–69. https://doi.org/10.1038/nprot.2007.514 PMID: 18193022.

88. Lauter G, Soll I, Hauptmann G. Multicolor fluorescent in situ hybridization to define abutting and overlapping gene expression in the embryonic zebrafish brain. Neural Dev. 2011; 6:10. Epub 2011/04/07. https://doi.org/10.1186/1749-8104-6-10 PMID: 21466670; PubMed Central PMCID: PMC3088888.

89. Vize PD, McCoy KE, Zhou X. Multichannel wholemount fluorescent and fluorescent/chromogenic in situ hybridization in Xenopus embryos. Nature protocols. 2009; 4(6):975–83. Epub 2009/06/06. https://doi.org/10.1038/nprot.2009.69 PMID: 19498377.

90. Yu L, Lam JC, Guo Y, Wu RS, Lam PK, Zhou B. Parental transfer of polybrominated diphenyl ethers (PBDEs) and thyroid endocrine disruption in zebrafish. Environ Sci Technol. 2011; 45(24):10652–9. Epub 2011/11/02. https://doi.org/10.1021/es2026592 PMID: 22039834.

91. Babaei F, Ramalingam R, Tavendale A, Liang Y, Yan LSK, Ajuh P, et al. Novel Blood Collection Method Allows Plasma Proteome Analysis from Single Zebrafish. Journal of proteome research. 2013; 12 (4):1580–90. https://doi.org/10.1021/pr3009226 PMID: 23413775

92. Parichy DM, Elizondo MR, Mills MG, Gordon TN, Engeszer RE. Normal table of postembryonic zebrafish development: staging by externally visible anatomy of the living fish. Dev Dyn. 2009; 238(12):2975–3015. Epub 2009/11/06. https://doi.org/10.1002/dvdy.22113 PMID: 19891001; PubMed Central PMCID: PMCPmc3030279.